Interfacing Superconducting Quantum Processors with Cryogenic Digital Circuitry

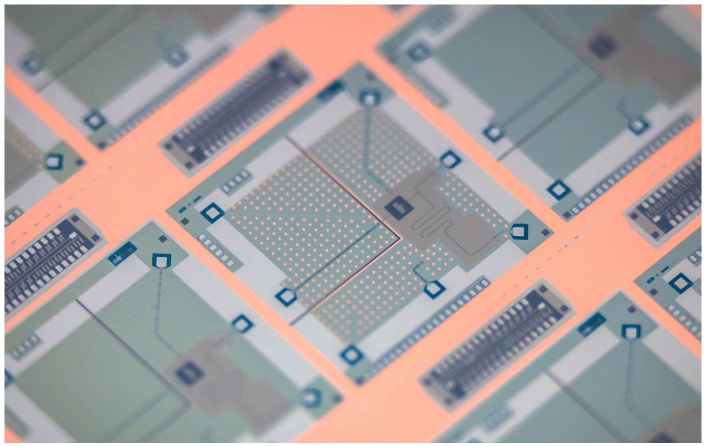

Britton L. T. Plourde
Syracuse University

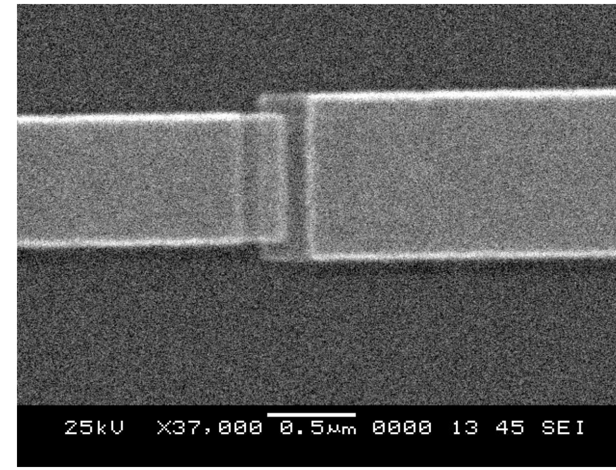

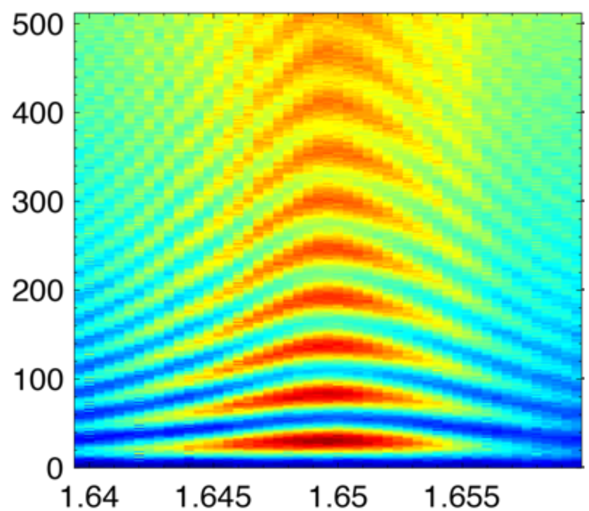

Rochester Institute of Technology
Photonics for Quantum Workshop
January 25, 2019

Acknowledgments

J. Nelson, C. Howington, K. Dodge,
A. Ballard, M. Hutchings, J. Ku
Syracuse University

M. Beck, E. Leonard, A. Opremcak, I. Pechenezhskiy,
M. Vavilov, R. McDermott
University of Wisconsin, Madison

L. Govia, P. Liebermann, E. Pritchett, F. Wilhelm
Saarland University

A. Kirichenko, J. Walter, D. Yohannes, O. Mukhanov
SeeQC (Hypres, Inc.)

Superconducting qubits

- 10^5 improvement in qubit performance
- Promising architecture for quantum information processors

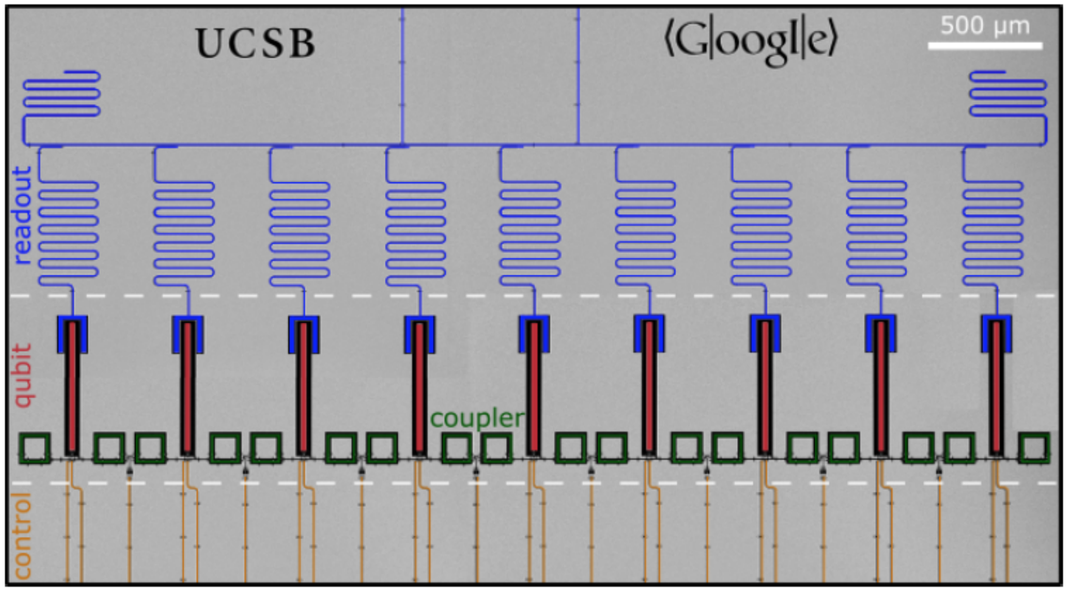

*C. Neill et al., Science (2018)

*Devoret & Schoelkopf (2013)

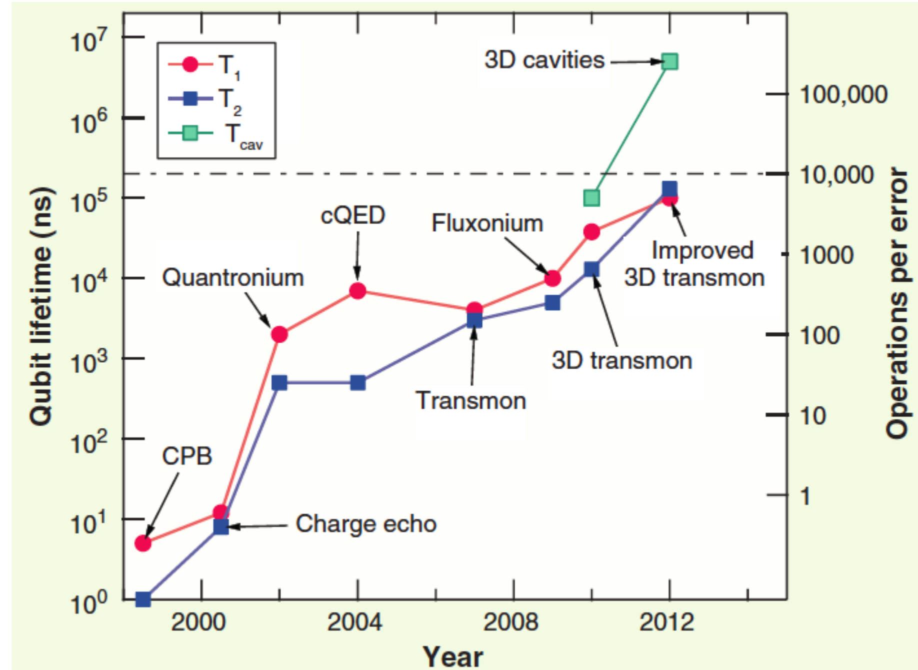

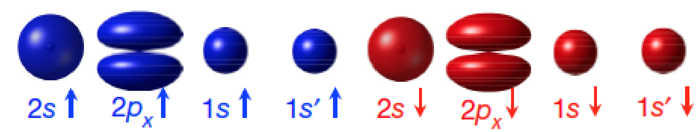

- Quantum optics with microwave photons
- Nodes for quantum network? — need microwave-to-optical transducer…

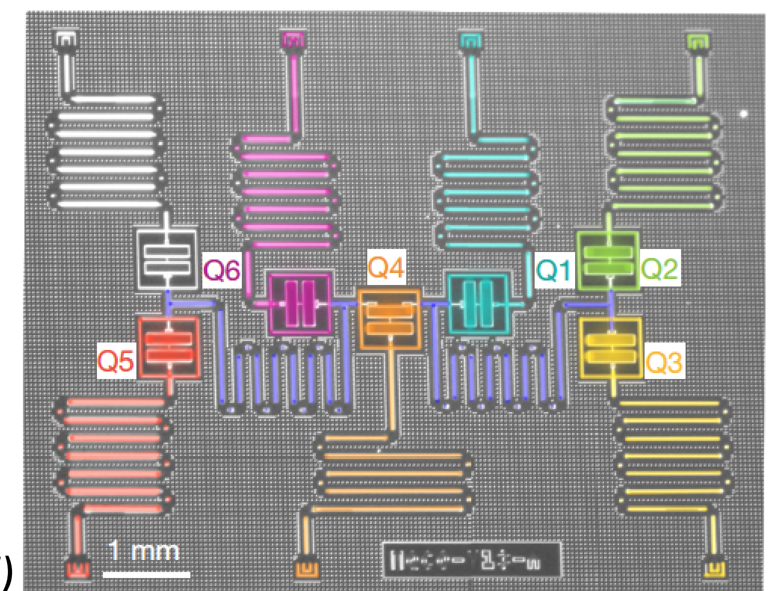

IBM

*A. Kandala et al., Nature (2017)

Outstanding challenges for building large systems of superconducting qubits

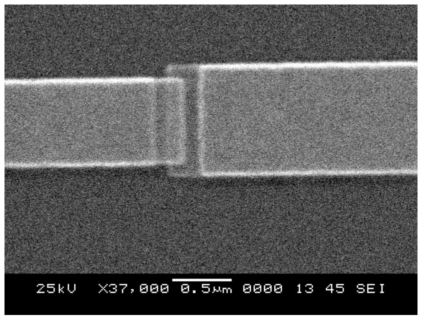

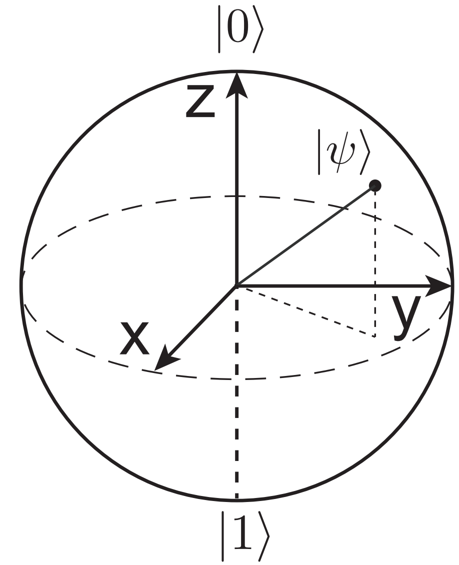

- Qubit coherence
- Spread in qubit parameters
- Frequency crowding
- Hardware requirements for qubit control
- Hardware requirements for qubit state readout

⋮

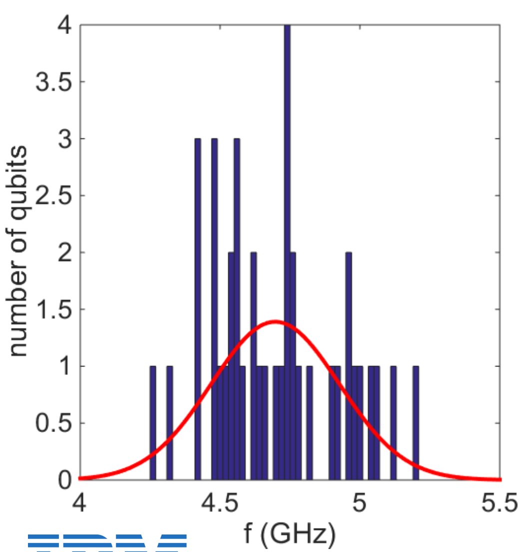

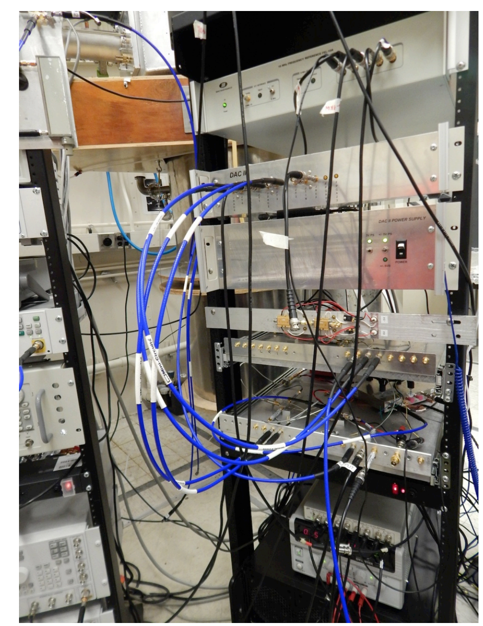

Basics of superconducting qubits

*Need a low-loss **anharmonic** oscillator at low-T*

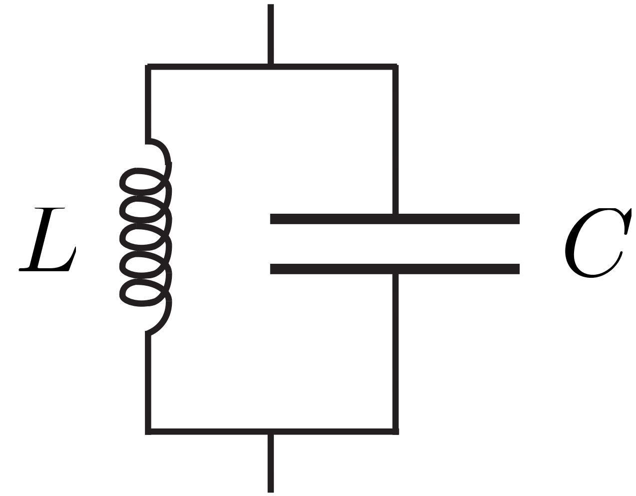

- Use a Josephson junction to form a ***superconducting*** nonlinear inductor

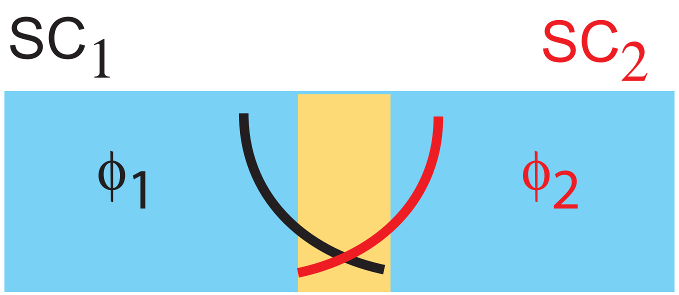

$$\phi = \phi_2 - \phi_1$$

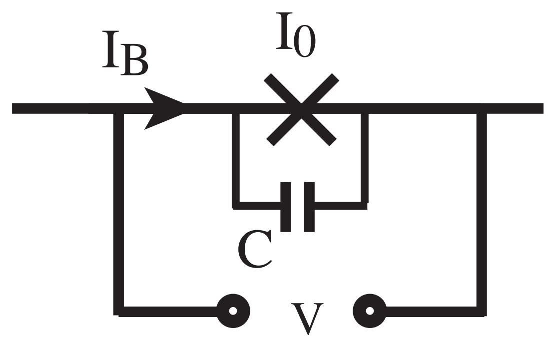

$$L_J = \frac{\Phi_0}{2\pi\sqrt{I_0^2 - I_B^2}}$$

Transmon

**J. Koch et al., Phys. Rev. A, 76, 042319 (2007)*

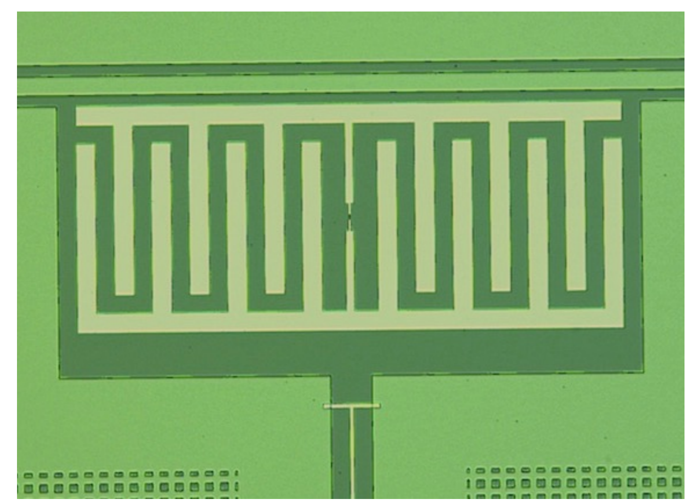

Microwave-based qubit control

Rabi oscillations

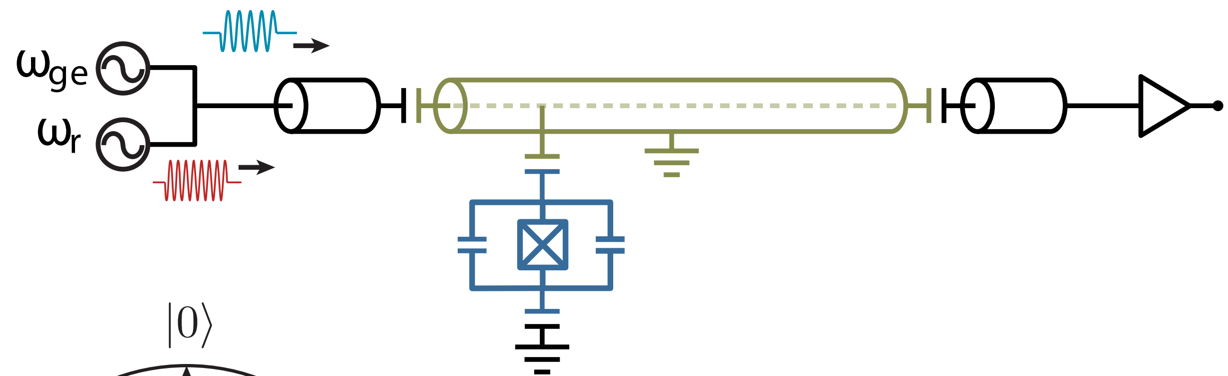

Vary duration of resonant qubit excitation pulse

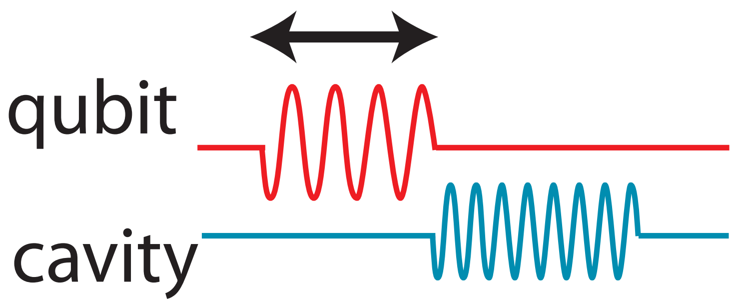

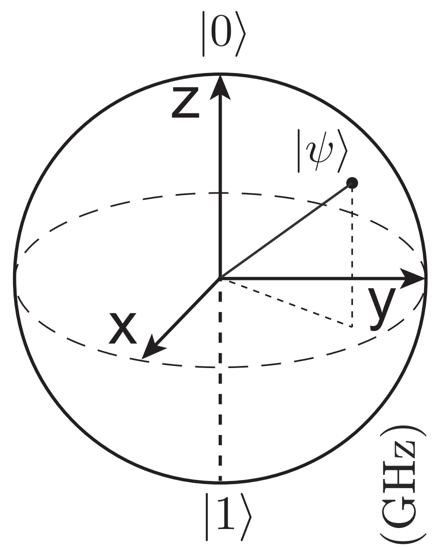

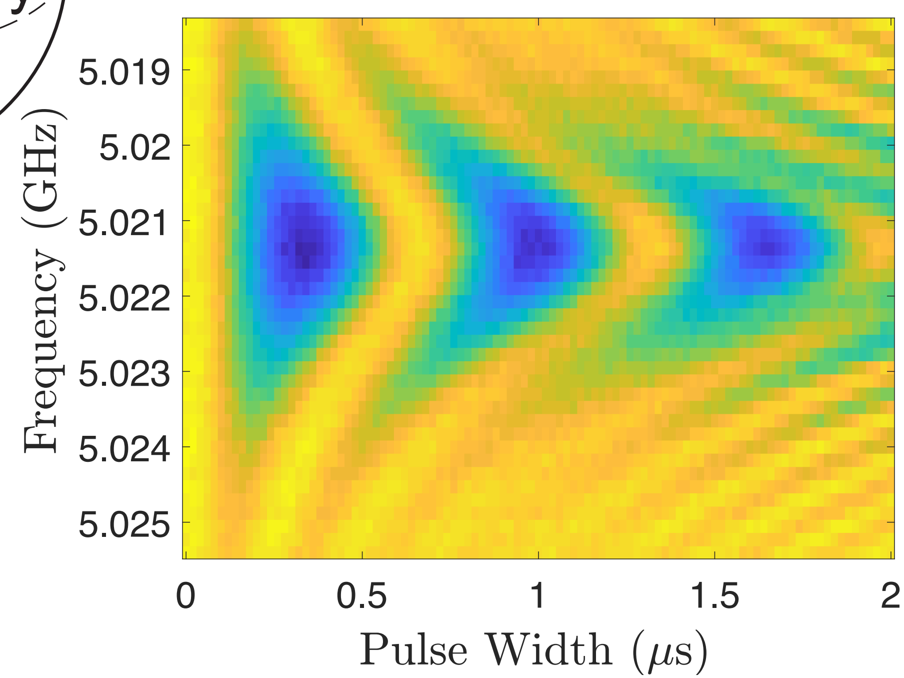

Adjust pulse duration and phase to generate qubit rotations on Bloch sphere

★ Works well, but significant hardware overhead…

Single-qubit gate fidelities > 99.9%

**R. Barends et al., Nature (2014)*
**S. Sheldon et al. PRA (2016)*

Dispersive measurements of qubit state

- Coupling between cavity and qubit results in dispersive shift of cavity

Dispersive shift: $2g^2/\Delta$

Cavity-qubit detuning: Δ

Blais et al., PRA 69, 062320 (2004)

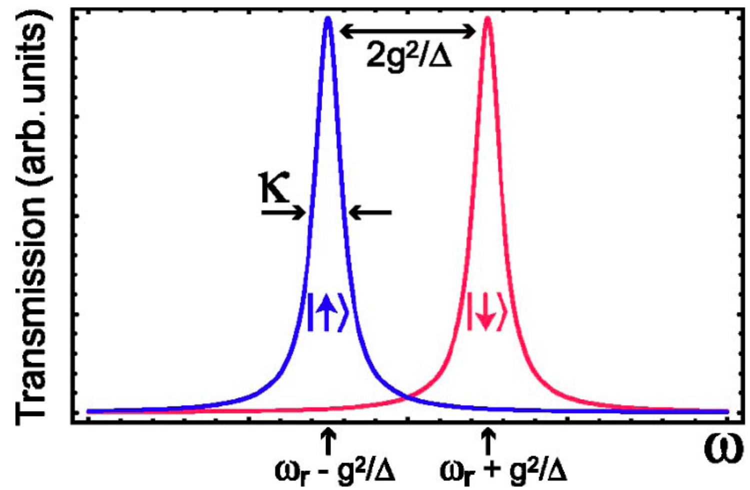

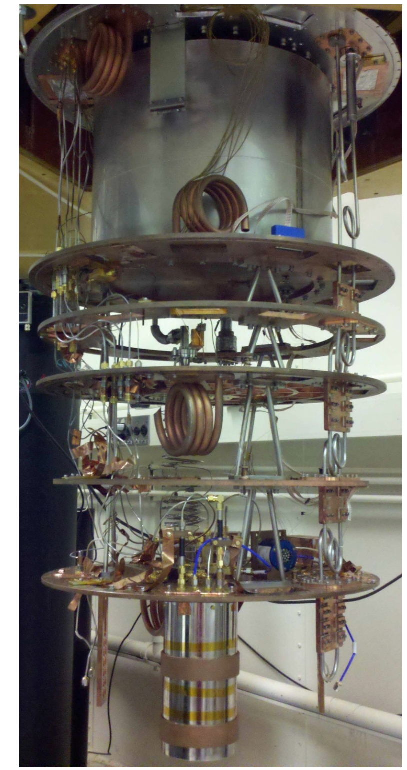

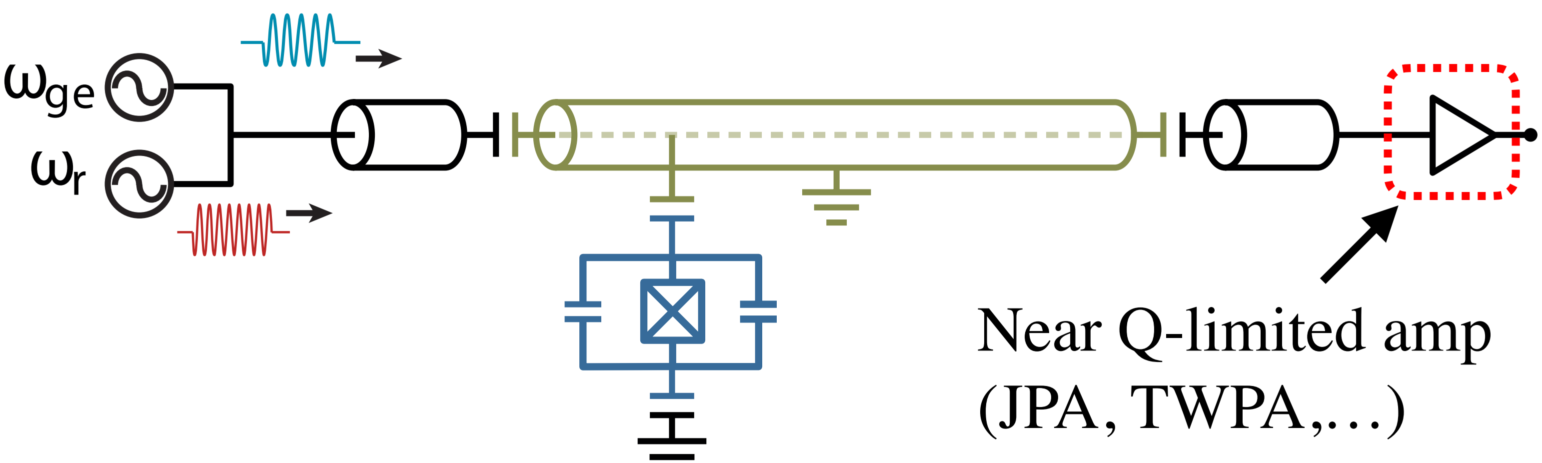

Near Q-limited amp (JPA, TWPA,…)

+

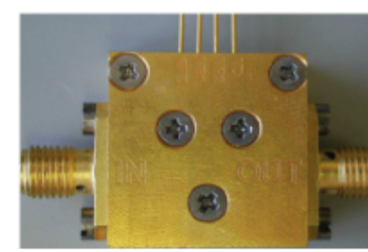

Cryogenic HEMT

★Works well, but significant hardware overhead…

Single-shot readout fidelities > 99% in under 500 ns

**T. Walter et al., PR Applied (2017)*

Reducing room-temperature hardware overhead

*McDermott *et al.*, Quant. Sci. Tech. 3, 024004 (2018)

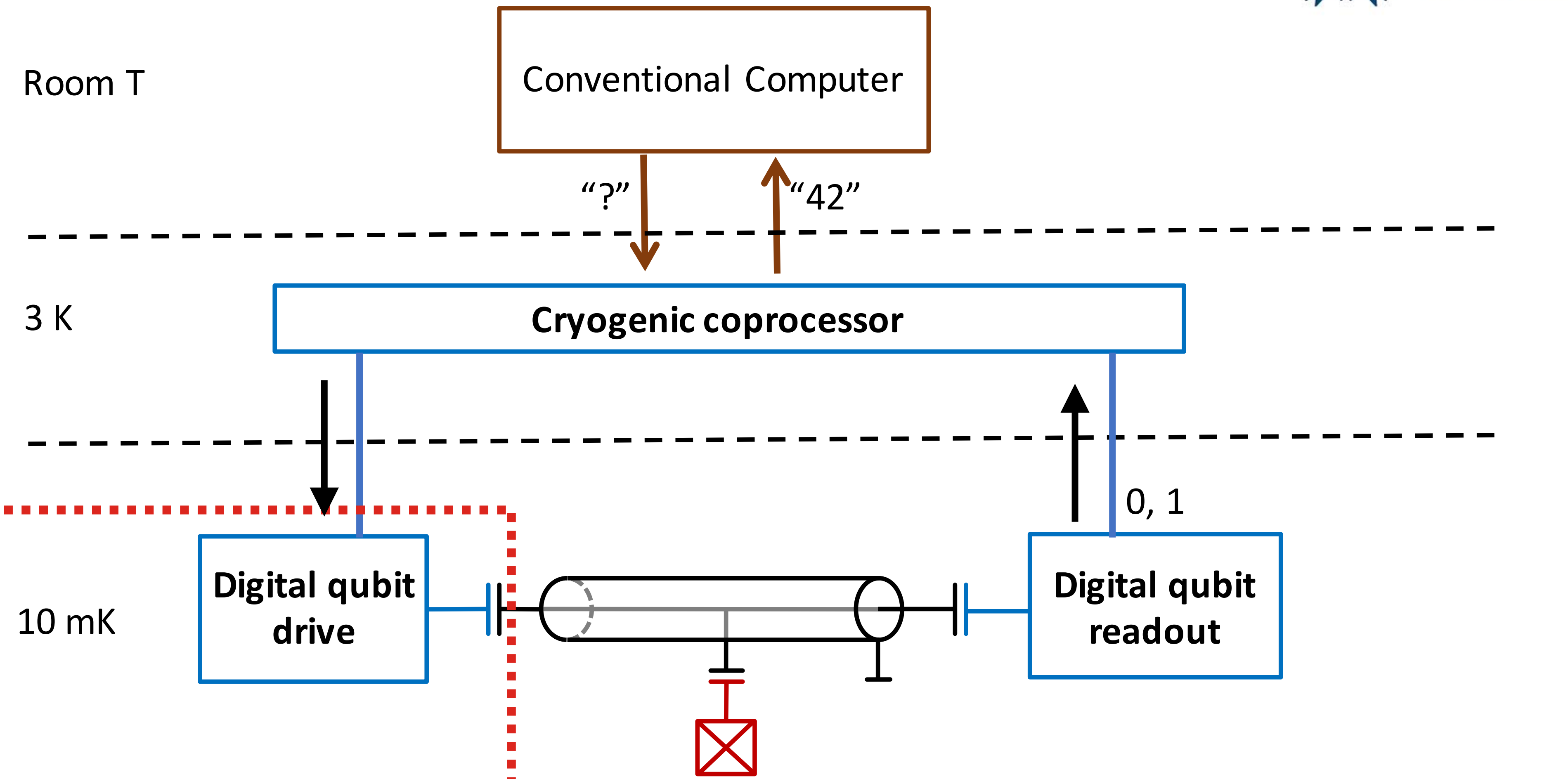

Cryogenic control of qubit state based on classical superconducting digital logic

Digital readout of qubit state based on microwave photon counting

Superconducting digital logic

- Classical superconducting digital logic — Single Flux Quantum (SFQ)

*Likharev and Semenov, *IEEE Trans. Appl. Supercon. 1991*

- Logical 1 (0) = presence (absence) of propagating fluxon

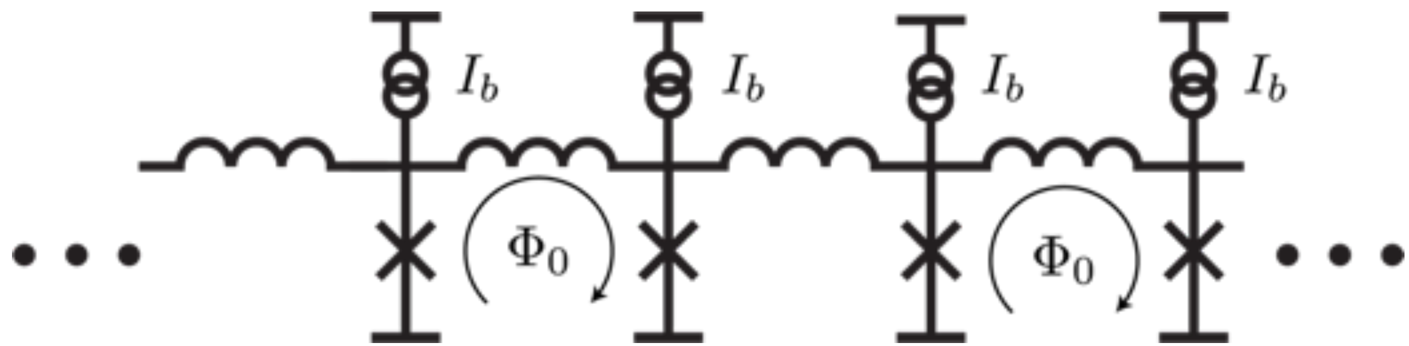

$$\Phi_0 = \frac{h}{2e}$$

- Low power consumption; high speed logic

$$\Phi_0 \approx 2\,\mathrm{mV} \times \mathrm{ps}$$

- Ongoing intensive effort to implement SFQ-based large-scale processor — IARPA C3 program

$$V(t) = \frac{\Phi_0}{2\pi}\frac{\partial \delta}{\partial t}$$

*Manheimer, *IEEE Trans. Appl. Supercon. 2015*

On-chip digital control of qubits

- SFQ circuitry on same chip as qubits or flip-chip coupling

- Capacitively couple resonant train of narrow SFQ pulses to drive qubit rotations without microwaves

- Important to mitigate heating/ quasiparticles produced on-chip from operation of SFQ circuitry

*McDermott and Vavilov, *Phys. Rev. Applied 2014*

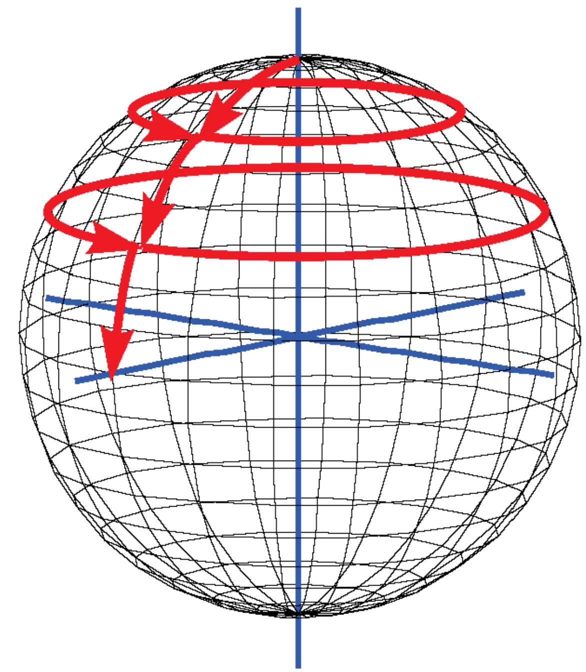

$$\delta\theta = C_c \Phi_0 \sqrt{\frac{2\omega_{01}}{\hbar C}}$$

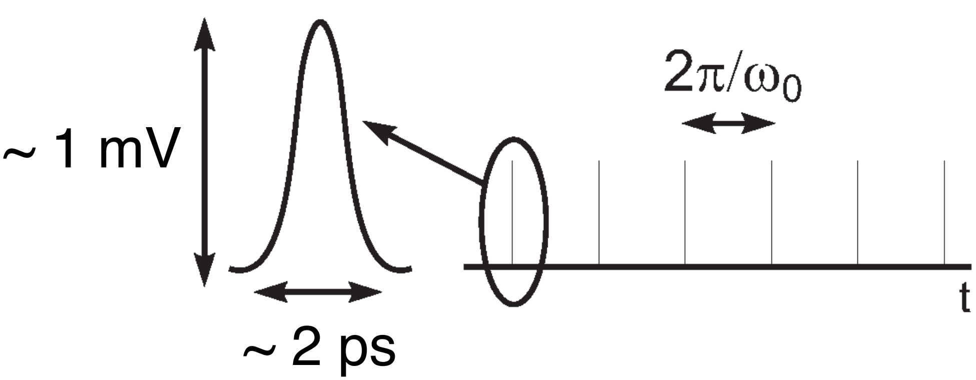

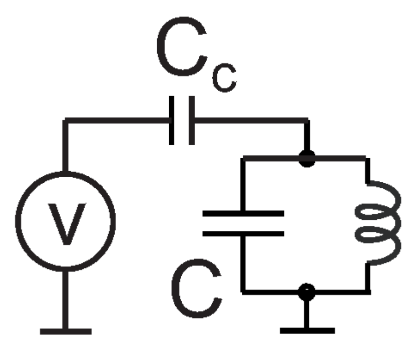

π rotation with ~100 pulses

~14 ns for 7 GHz qubit

Implementation of SFQ driver and qubits

- Collaborative hybrid fabrication
- High-Jc Nb/AlOx/Nb junctions from Wisconsin
- Low-Jc Al/AlOx/Al junctions from Syracuse

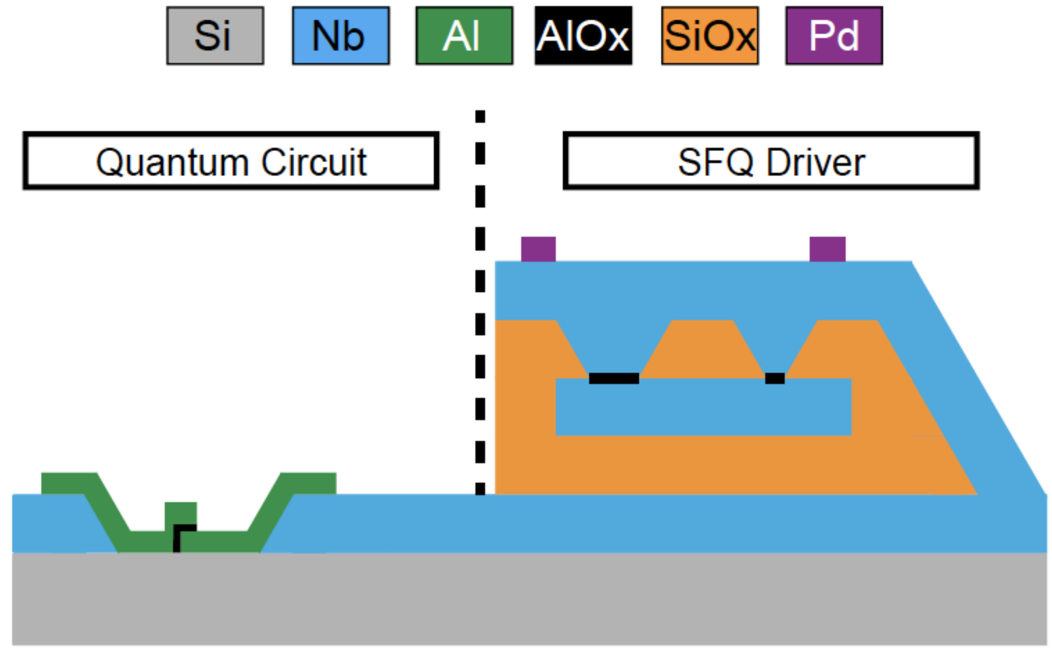

*Leonard *et al.*, Phys. Rev. Applied 11, 014009 (2019)

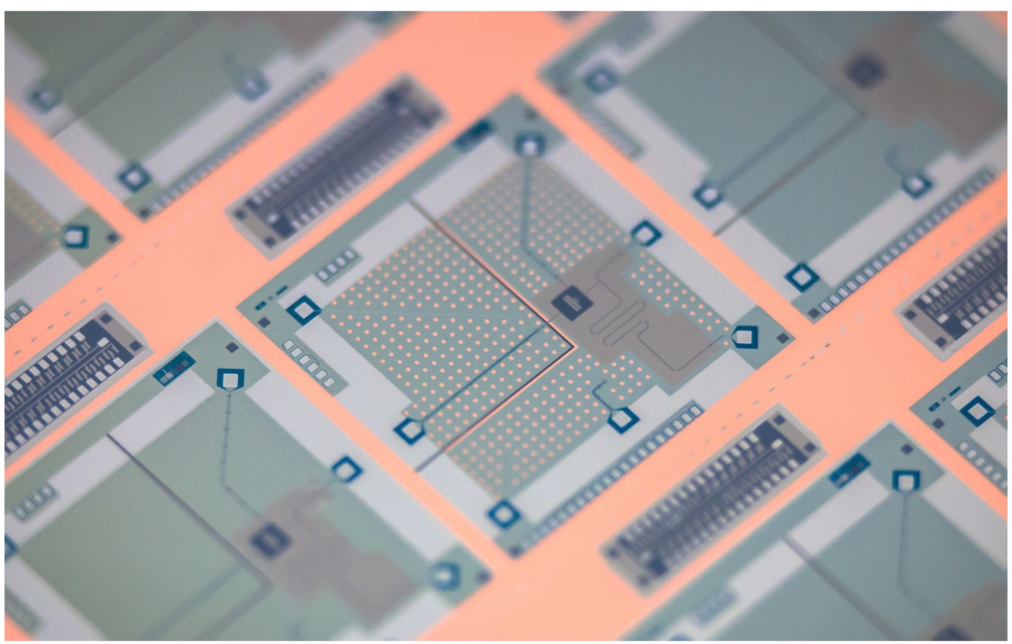

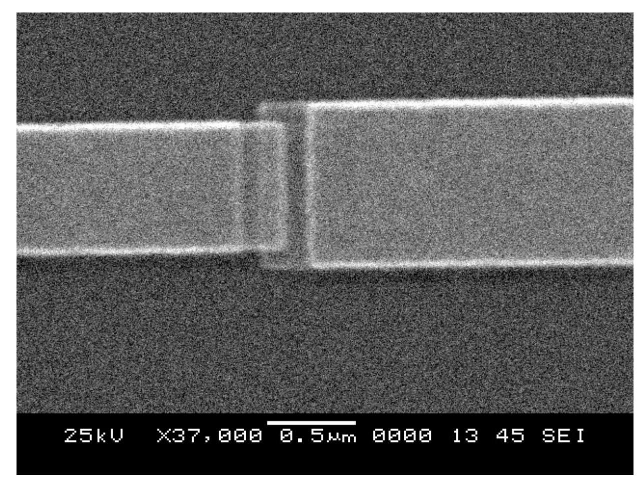

Layout of SFQ driver and qubit

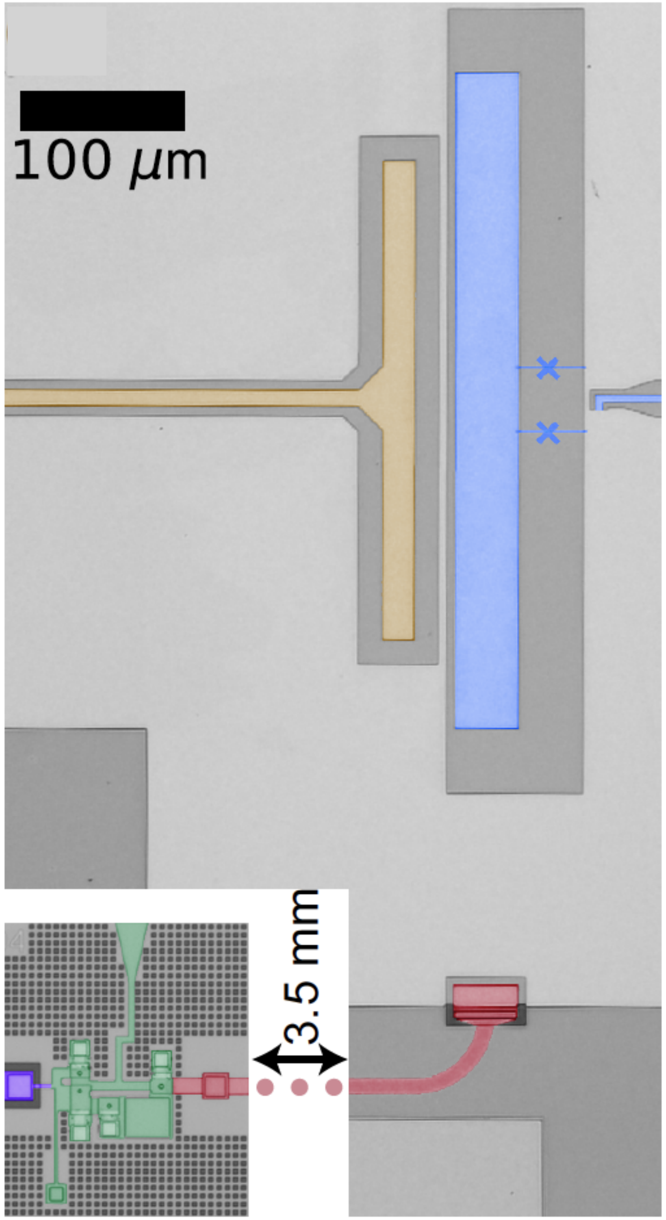

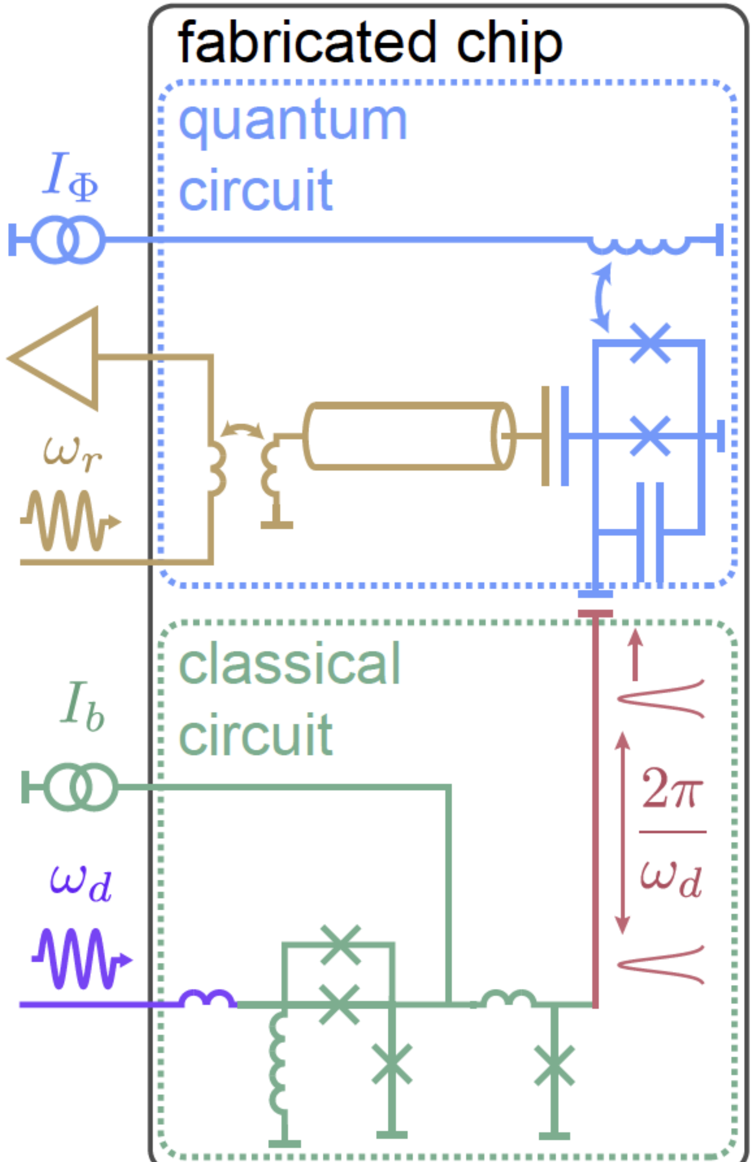

- Conventional heterodyne qubit readout
- Decent coherence

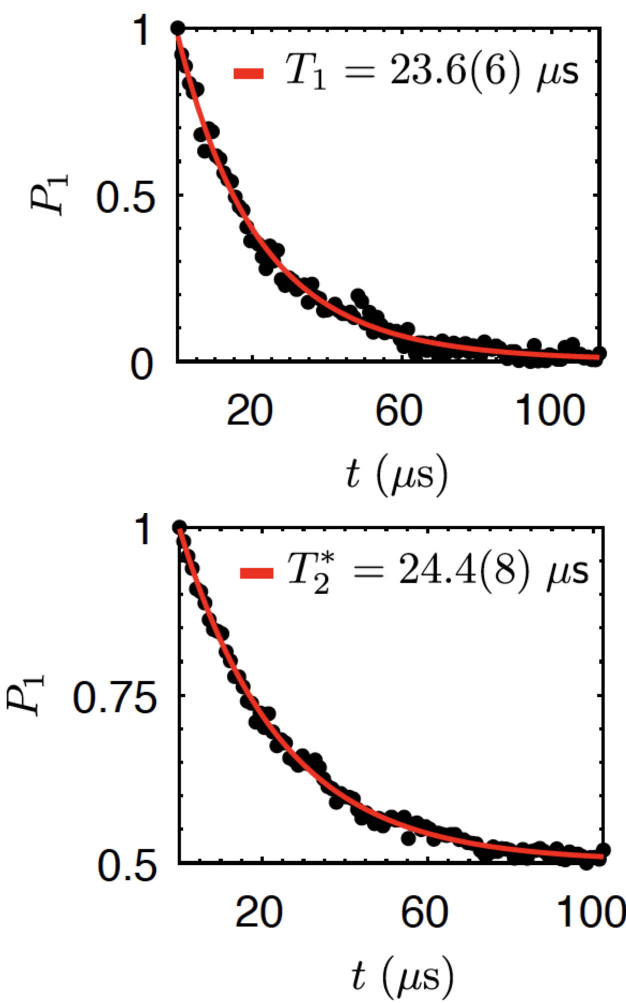

Qubit Rabi oscillations with SFQ pulses

- Bias qubit at upper sweet spot: $\omega_{10}/2\pi = 4.958\,\mathrm{GHz}$
- Send microwave pulses to trigger input of SFQ driver

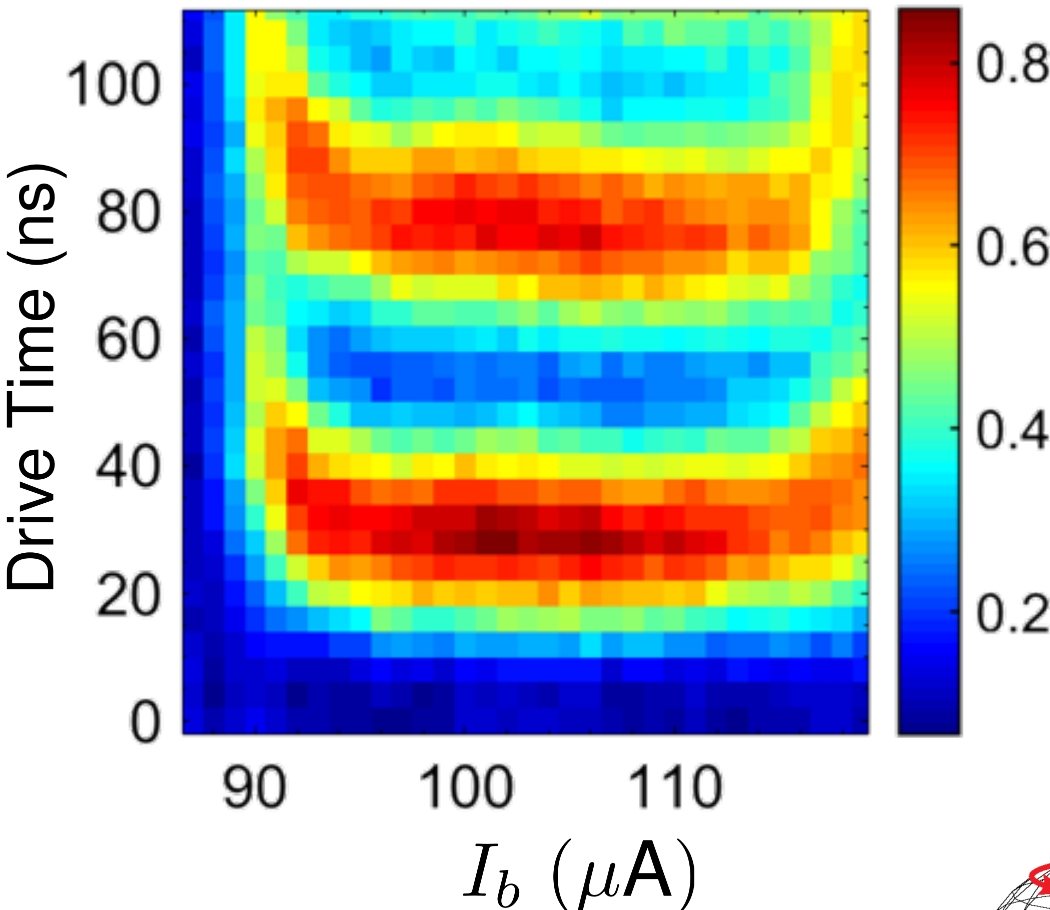

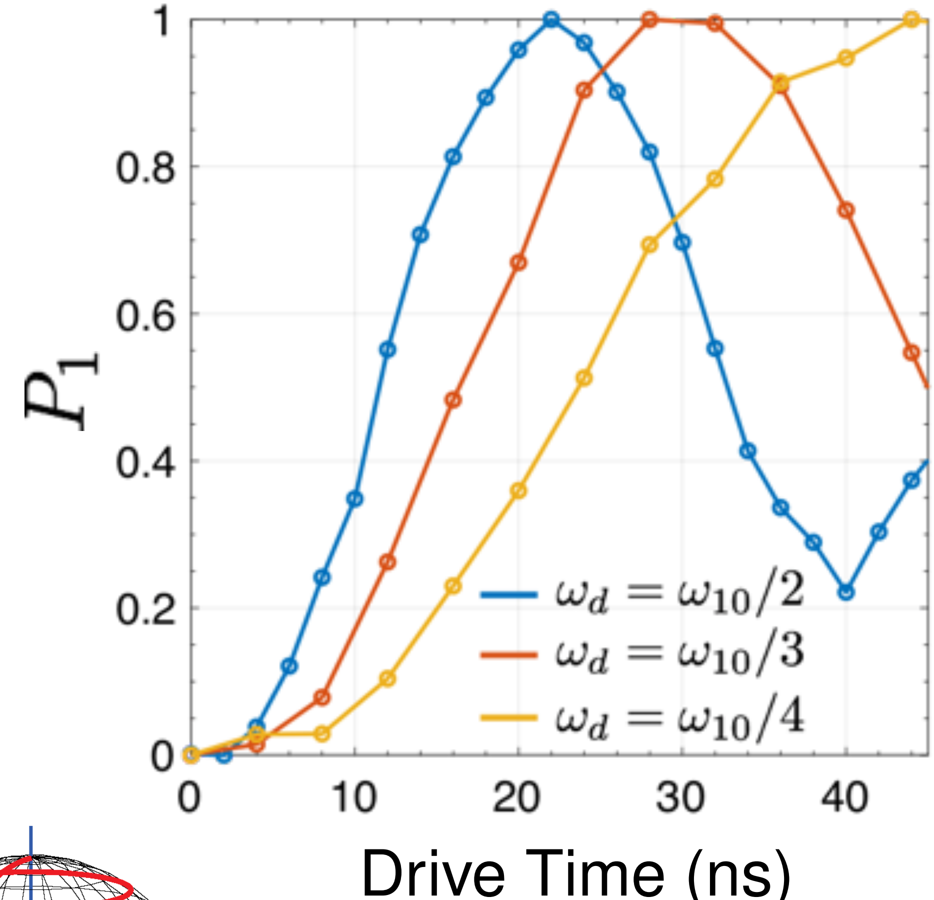

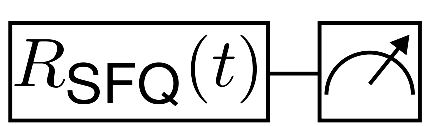

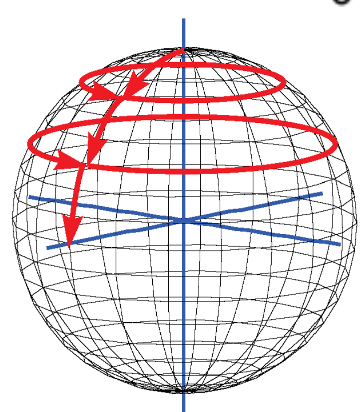

Drive SFQ circuit on subharmonic to avoid direct drive of qubit

Qubit Rabi oscillations at $\omega_{10}/3$

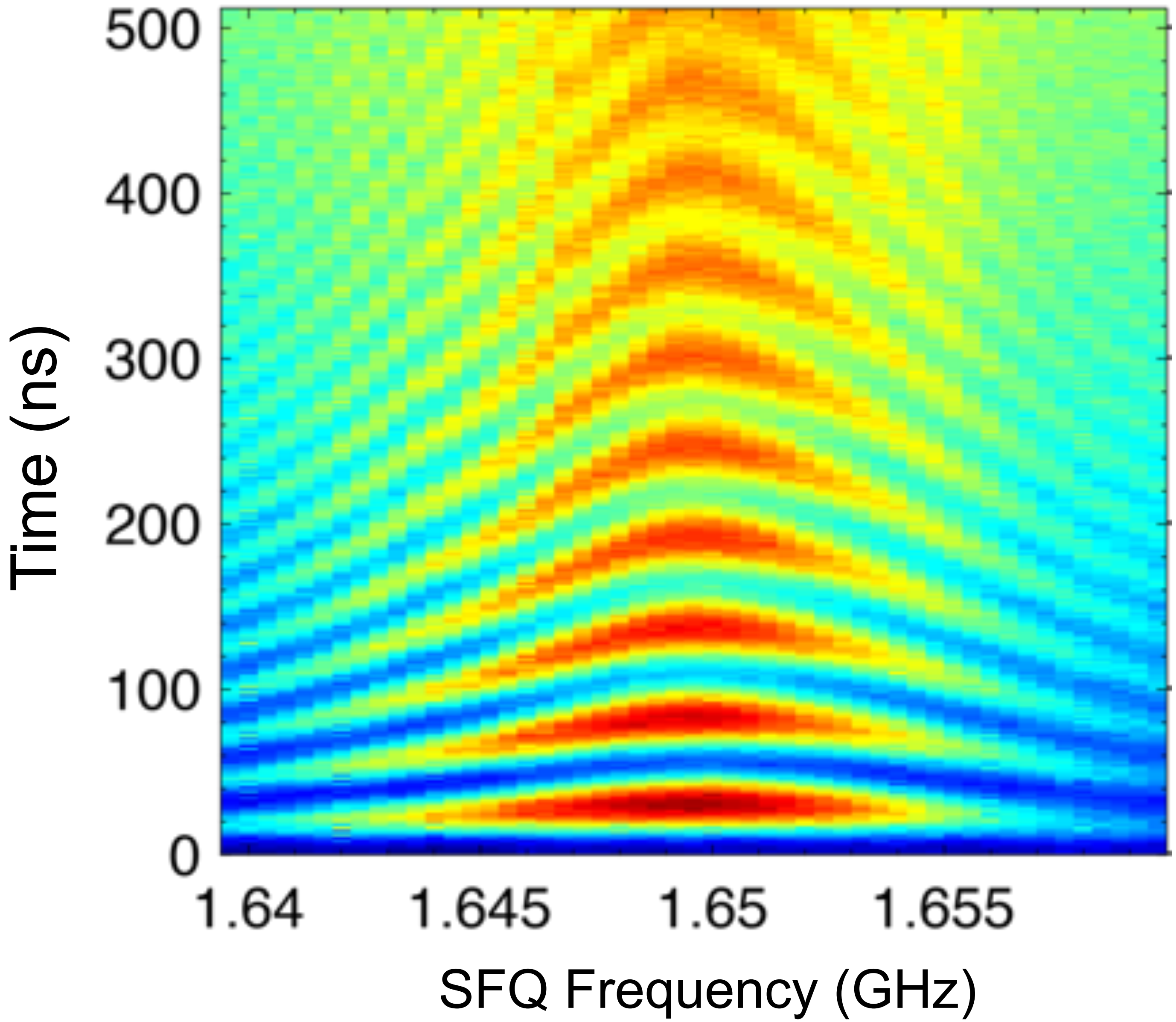

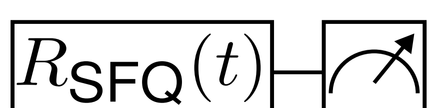

Orthogonal gates with SFQ pulses

$$\mathrm{RF}(t) = \cos[\underbrace{(\omega_{\mathrm{LO}} - \omega_{\mathrm{IF}})}_{\omega_d} t + \phi_d]$$

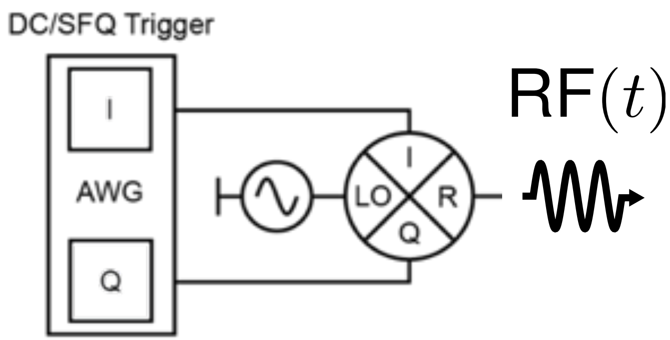

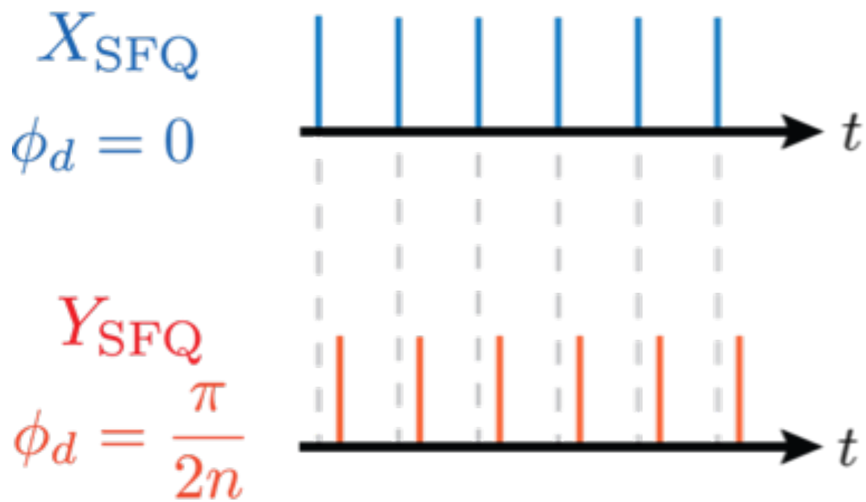

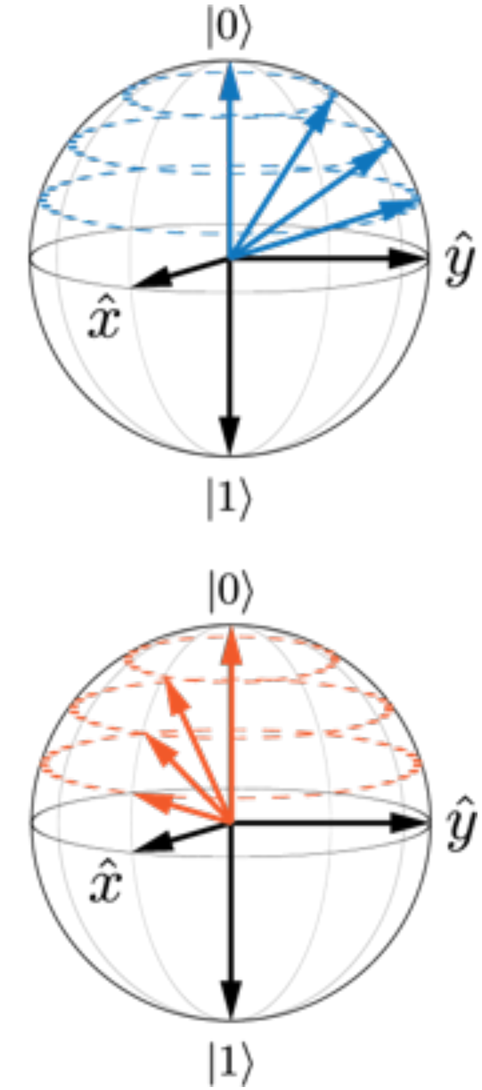

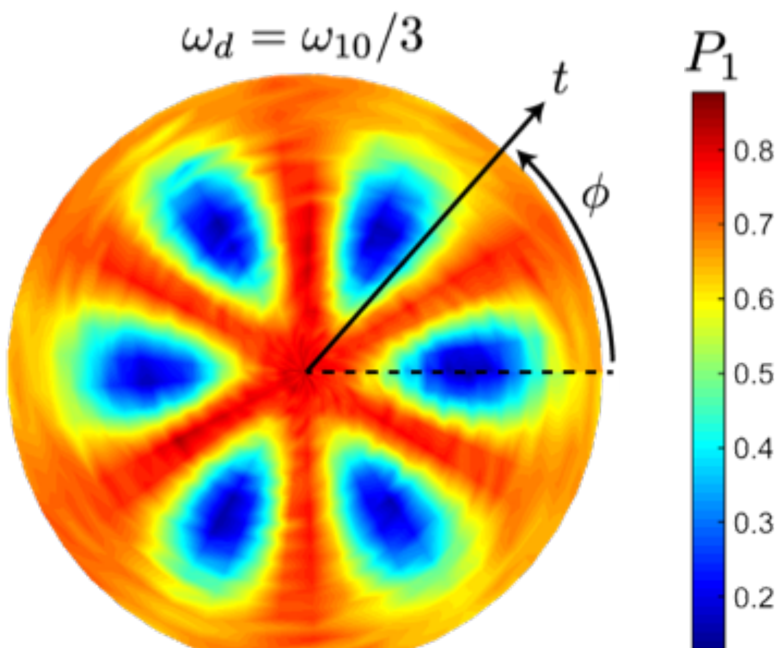

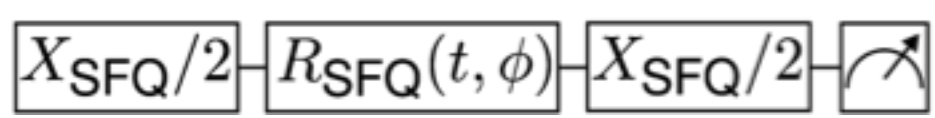

Characterizing SFQ-based gates

Randomized benchmarking

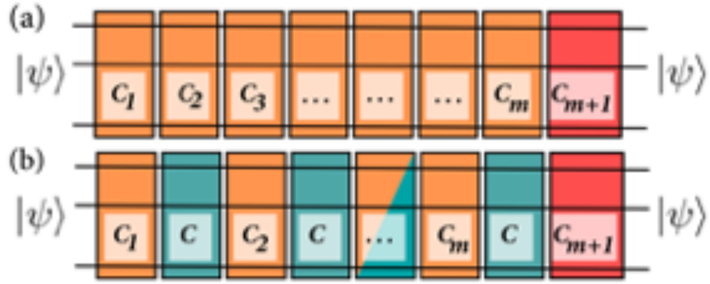

*Magesan *et al.*, PRL 109, 080505 (2012)

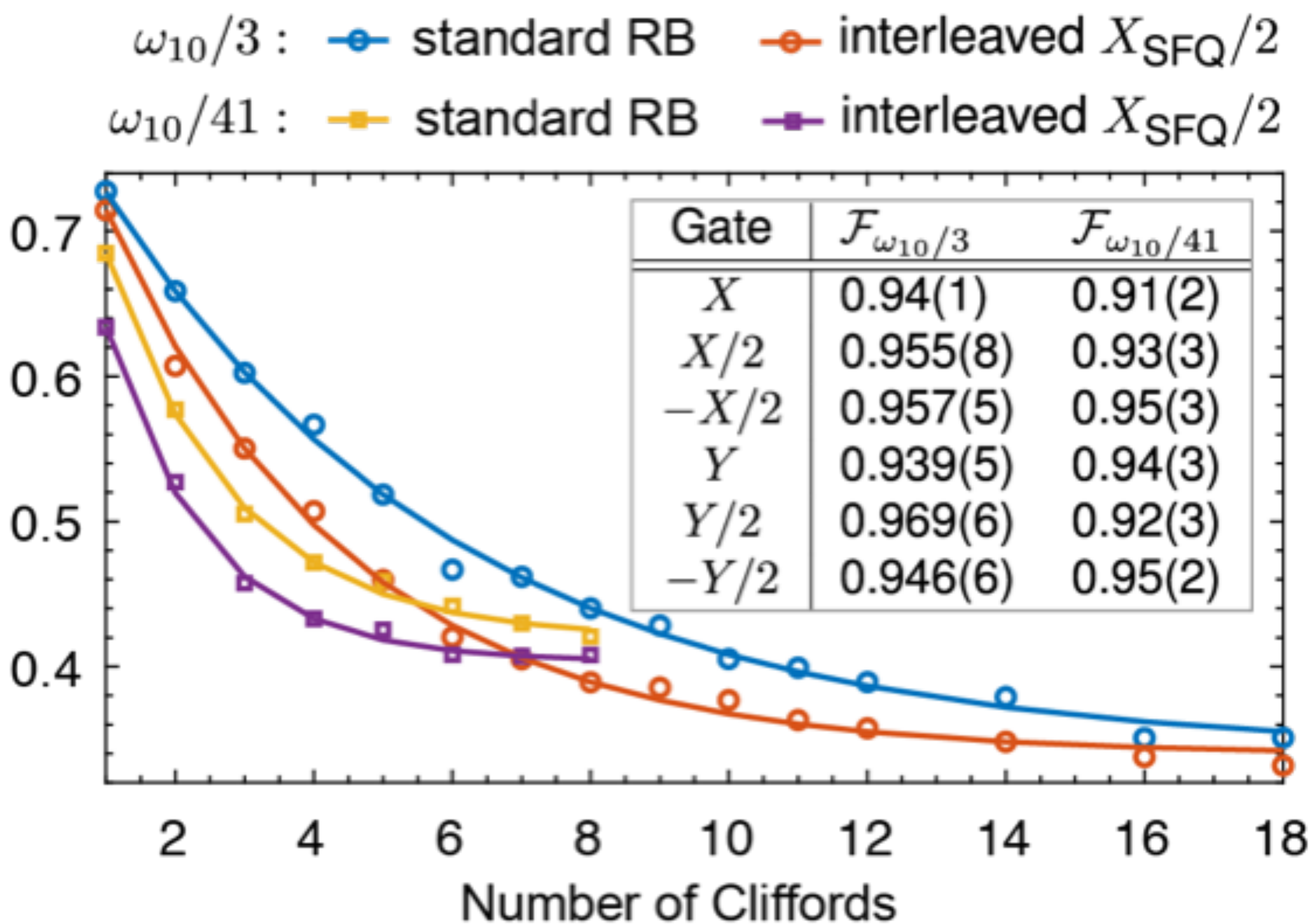

Gate	$\mathcal{F}_{\omega_{10}/3}$	$\mathcal{F}_{\omega_{10}/41}$
X	0.94(1)	0.91(2)
$X/2$	0.955(8)	0.93(3)
$-X/2$	0.957(5)	0.95(3)
Y	0.939(5)	0.94(3)
$Y/2$	0.969(6)	0.92(3)
$-Y/2$	0.946(6)	0.95(2)

Gate fidelities limited by on-chip quasiparticle generation

Quasiparticle poisoning

- Trigger SFQ driver off-resonant from qubit subharmonics
- Phase slips of SFQ junctions generate quasiparticles that poison qubit

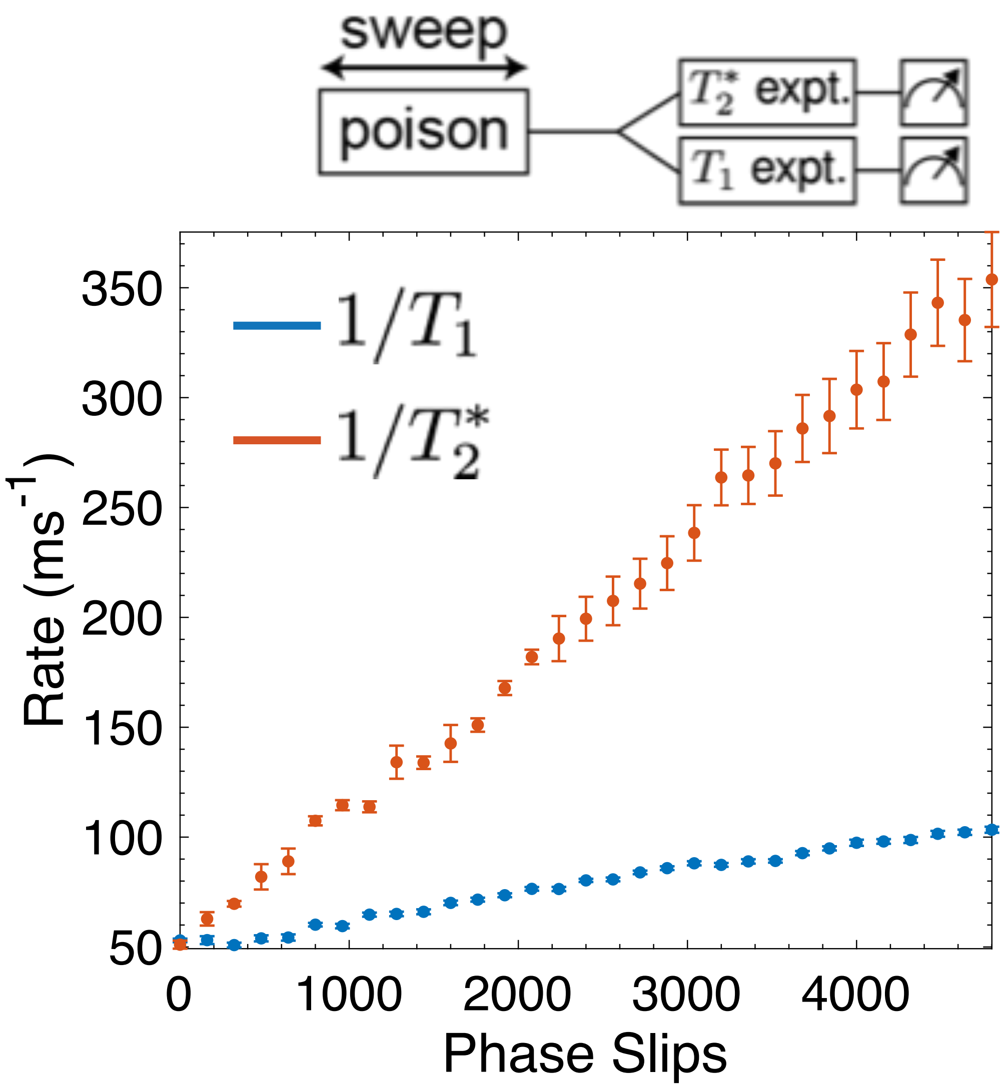

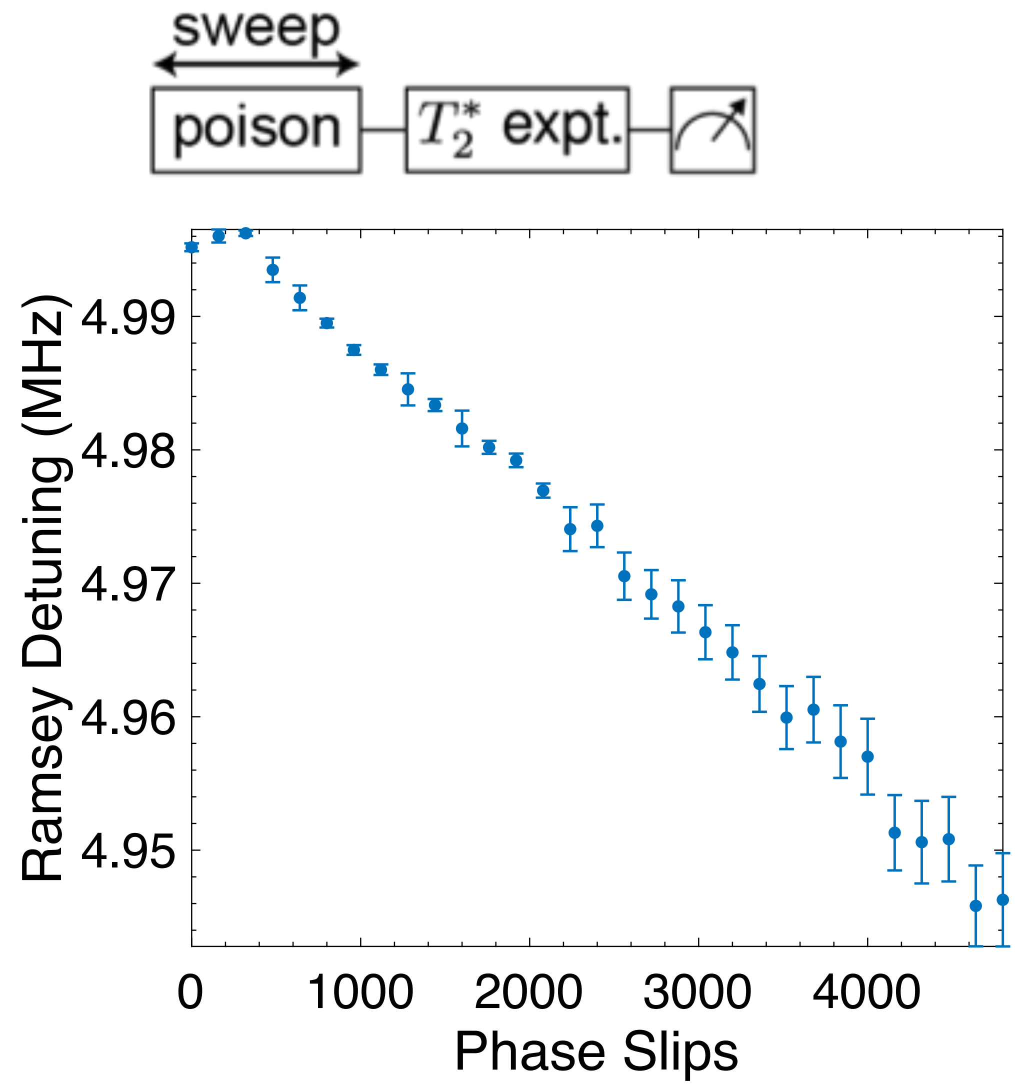

QP admittance: *Real → -enhanced dissipation

*Imaginary → -frequency shift

Mitigating quasiparticle poisoning

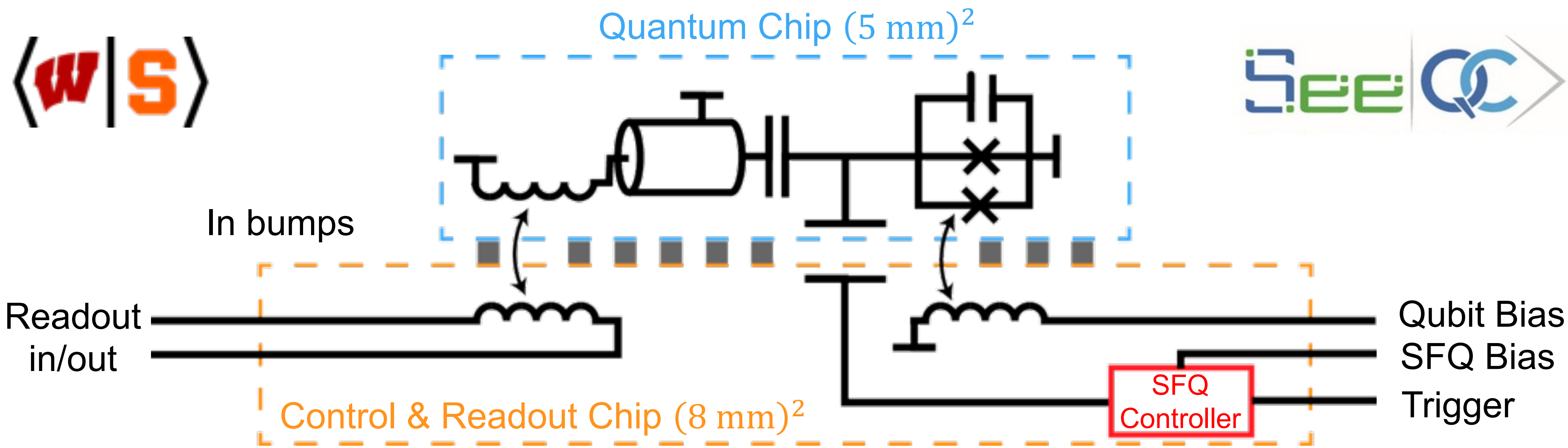

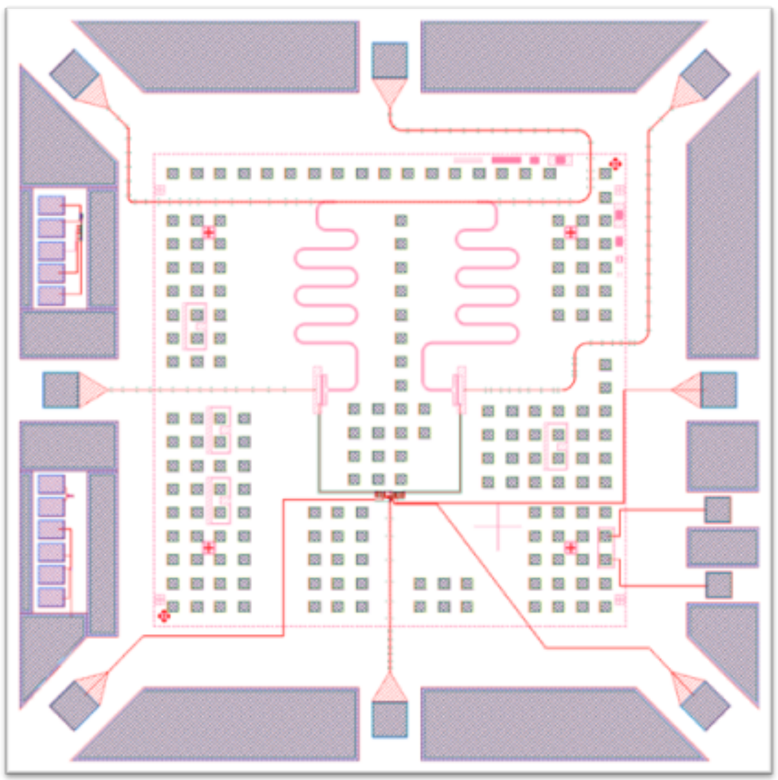

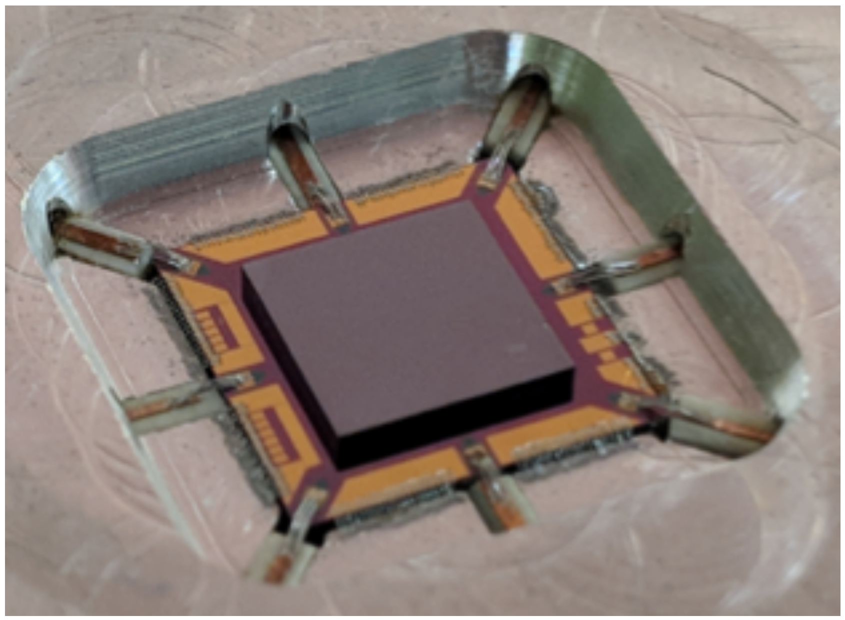

Multi-chip module: initial measurements

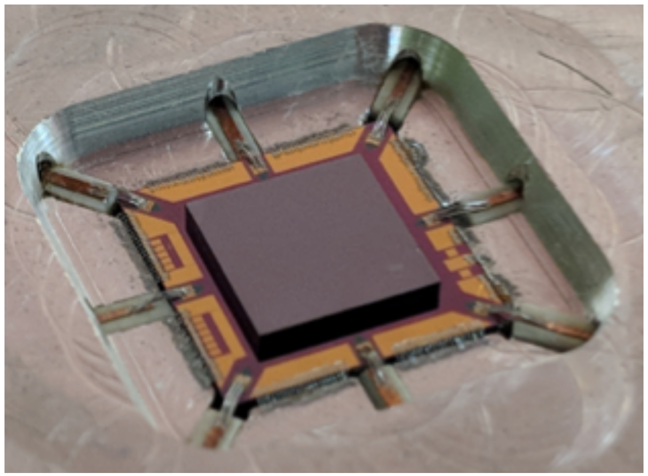

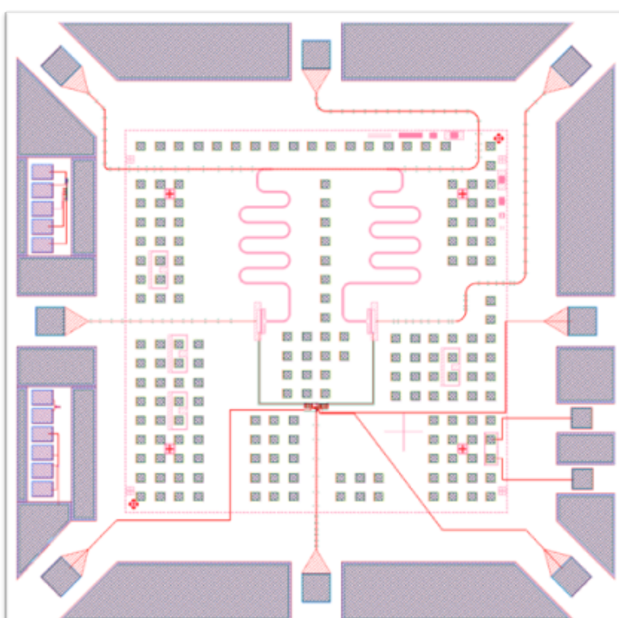

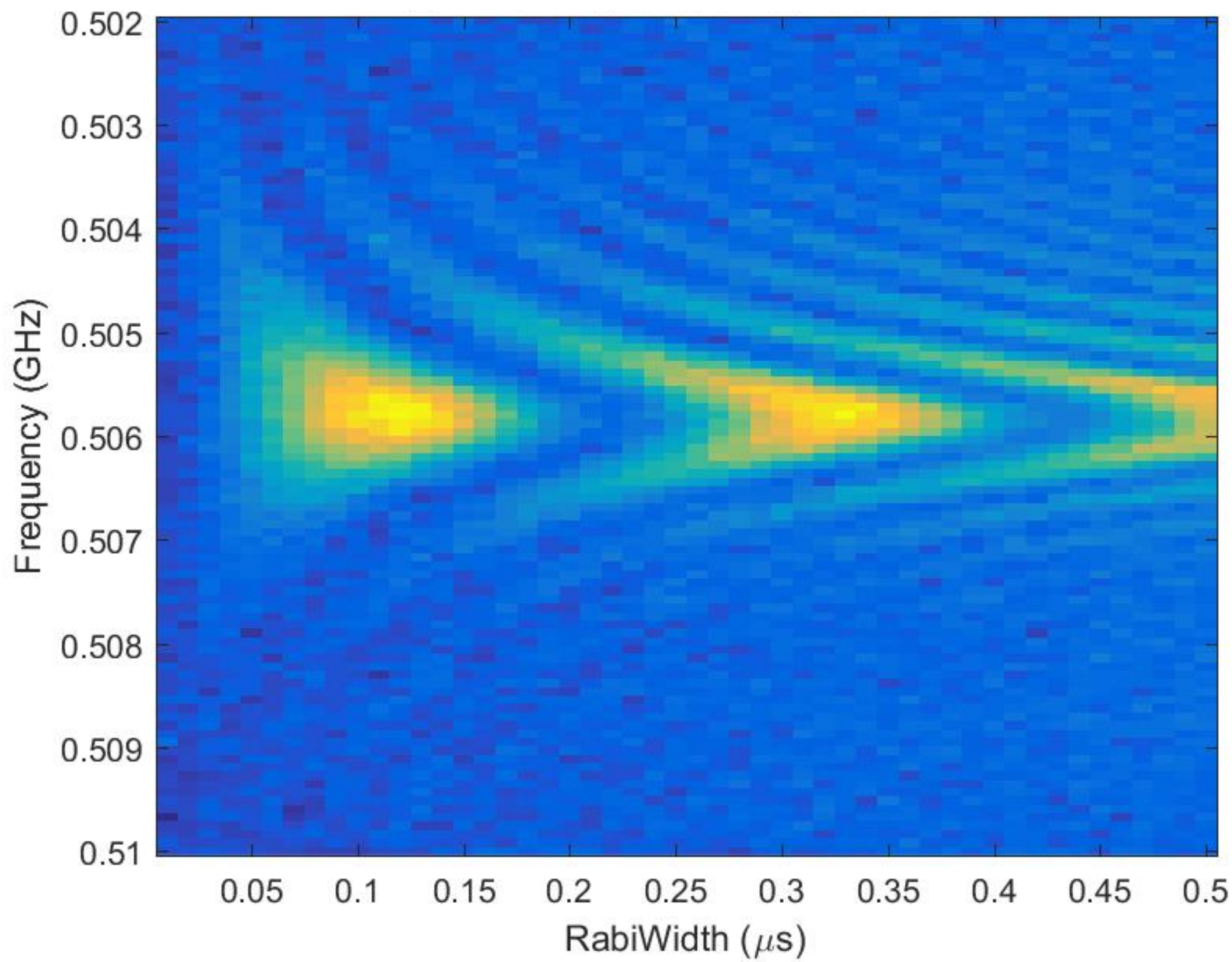

SFQ Pulse Pattern Generator

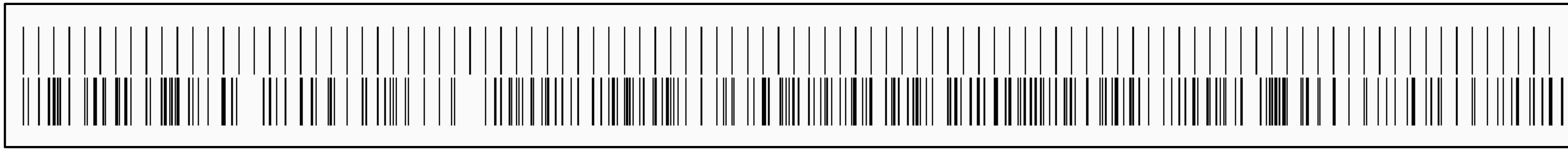

- For more accurate qubit control, need to be able to generate more complex patterns of SFQ pulses

P. Liebermann *et al.*, Phys. Rev. Appl. 6, 024022 (2016)

UNIVERSITÄT DES SAARLANDES

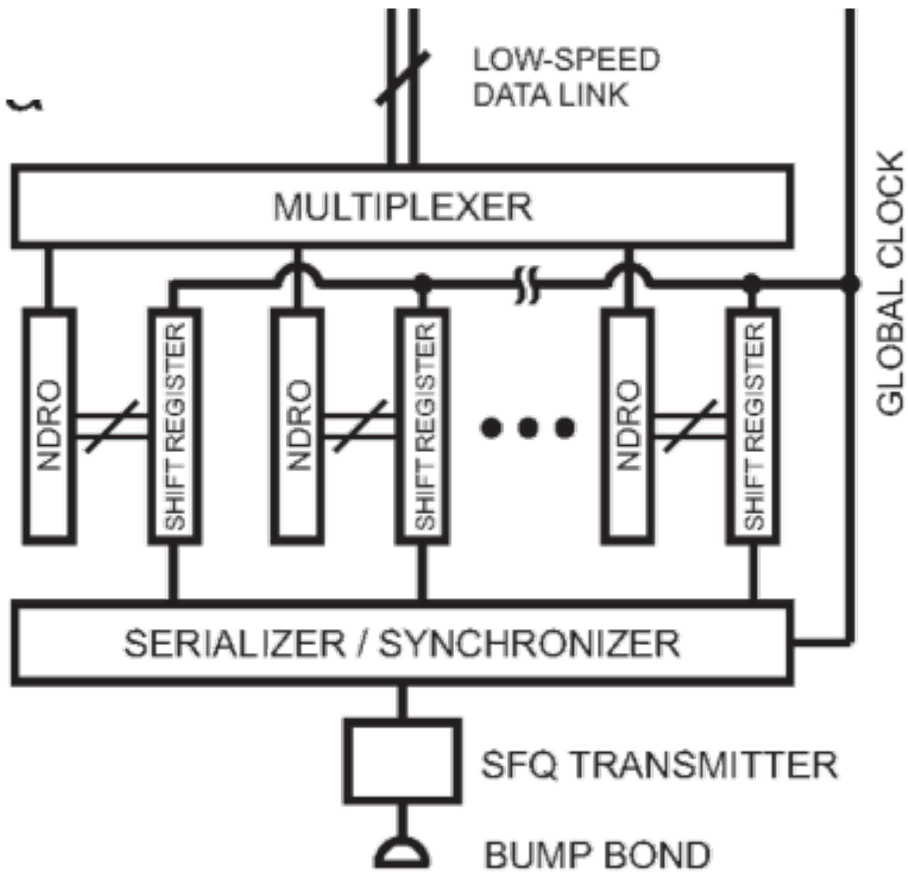

with O. Mukhanov, *SeeQC (Hypres, Inc.)*

- Single global clock (e.g., 30 GHz)
- Banks of shift registers to store/stream sequence (e.g., 10x200 bits)

Reducing room-temperature hardware overhead

*McDermott *et al.*, Quant. Sci. Tech. 3, 024004 (2018)

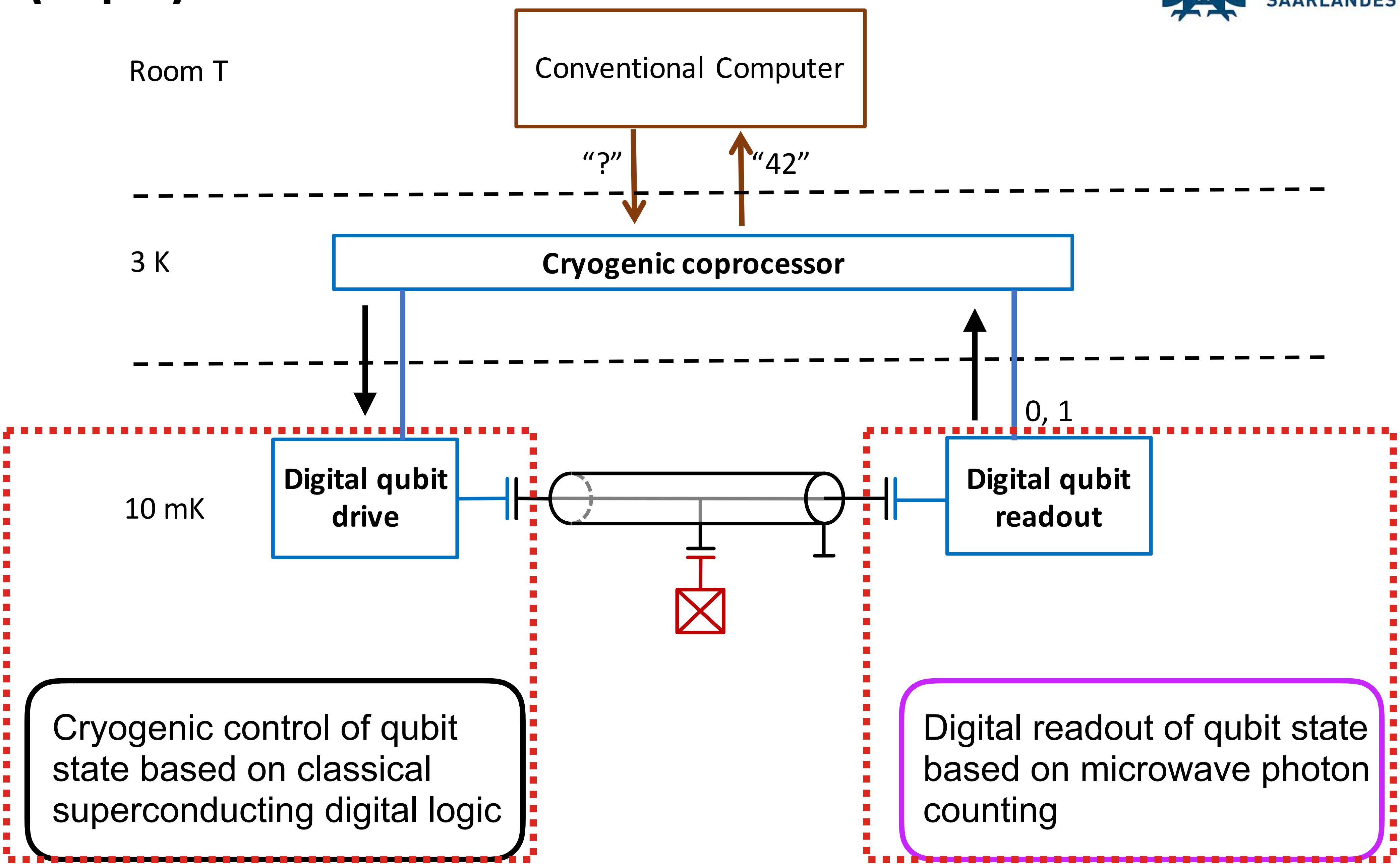

Digital Readout of Qubit with Josephson Photomultiplier

*Opremcak *et al.*, Science 361, 1239 (2018)

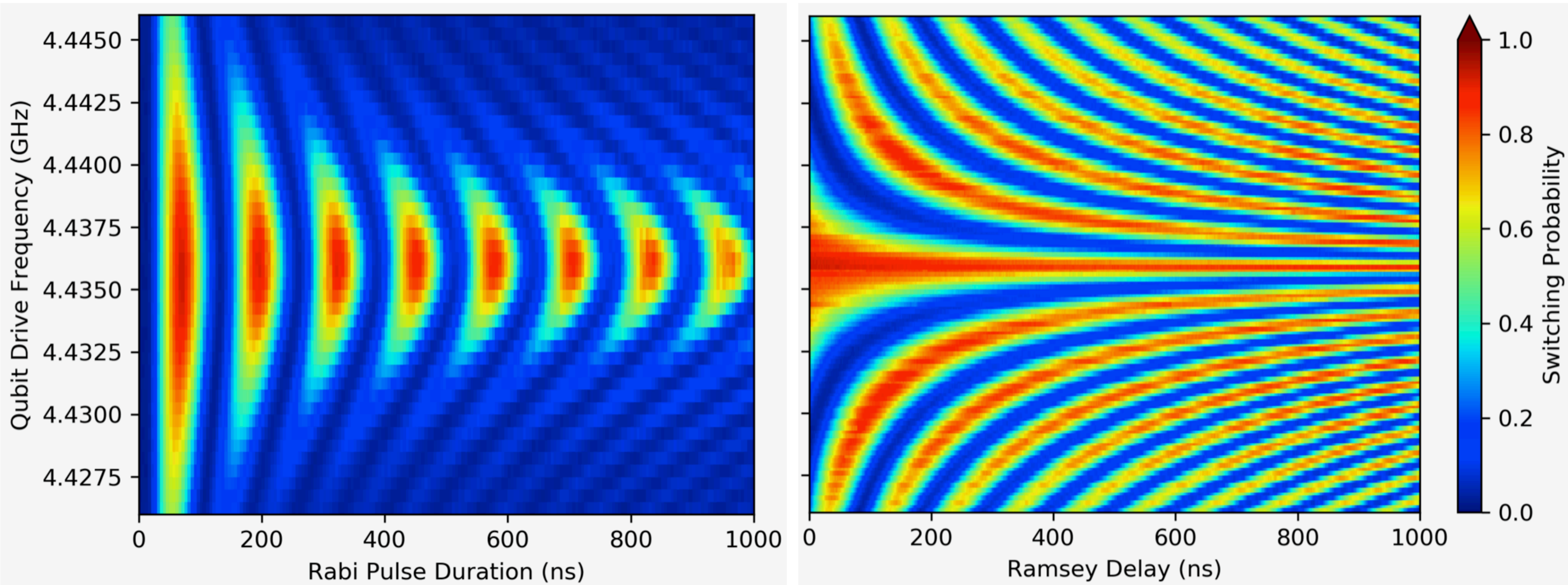

Raw measurement fidelity ≈ 92%

Quantum-Classical Interface

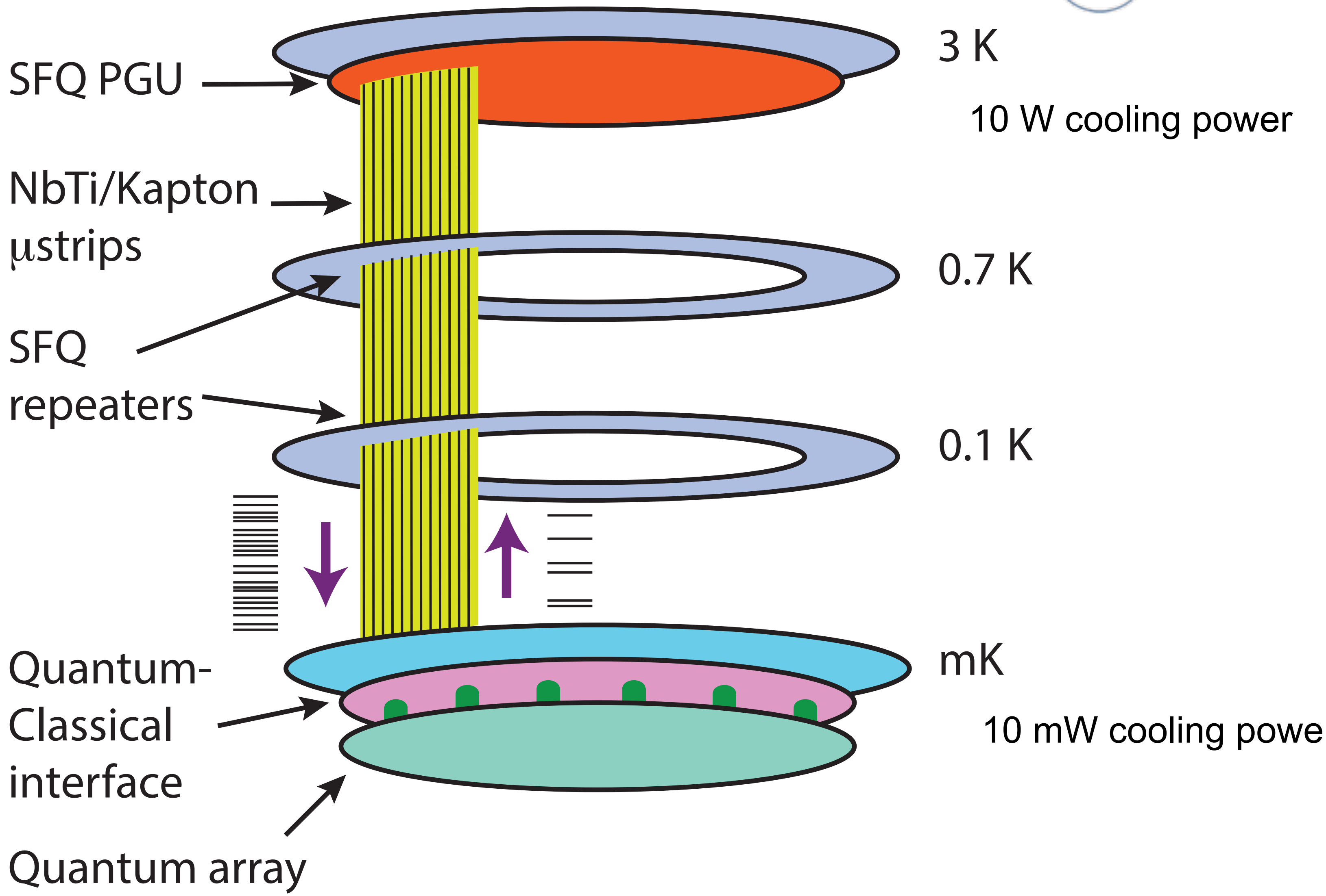

*McDermott *et al.*, Quant. Sci. Tech. 3, 024004 (2018)

Quantum layer = qubits and readout resonators only; minimal fab processing

Quantum-Classical interface layer = SFQ drivers; JPMs and SFQ output; flux bias lines

Summary

- Hardware challenges for scaling to large qubit arrays with conventional microwave-based control and readout

  *McDermott *et al.*, Quant. Sci. Tech. 3, 024004 (2018)

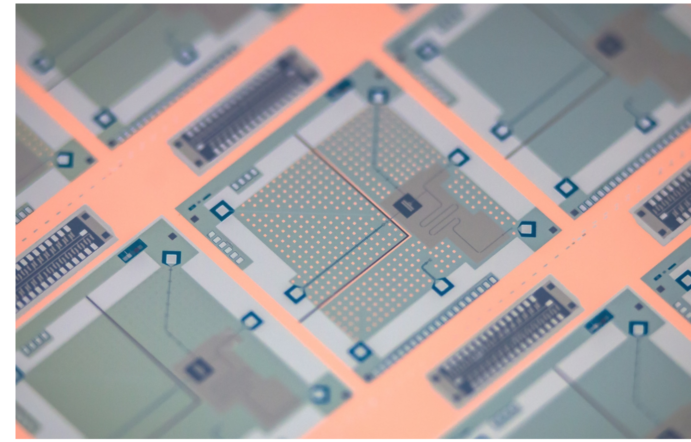

- SFQ-based qubit control without microwave pulses

  *Leonard *et al.*, Phys. Rev. Applied 11, 014009 (2019)

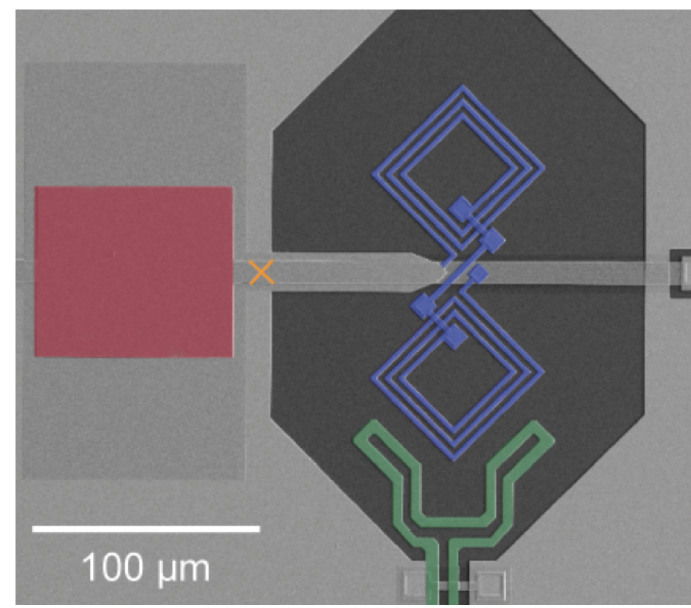

- Microwave photon counter JPMs for digital readout of qubit state

  *Opremcak *et al.*, Science 361, 1239 (2018)

Alternative approaches to dispersive readout in cQED

…by Amplification:

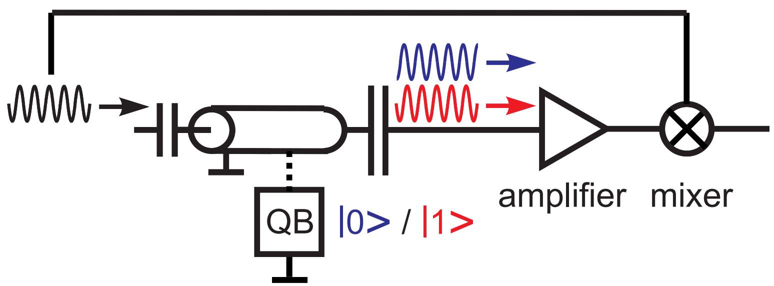

Coherent state discrimination

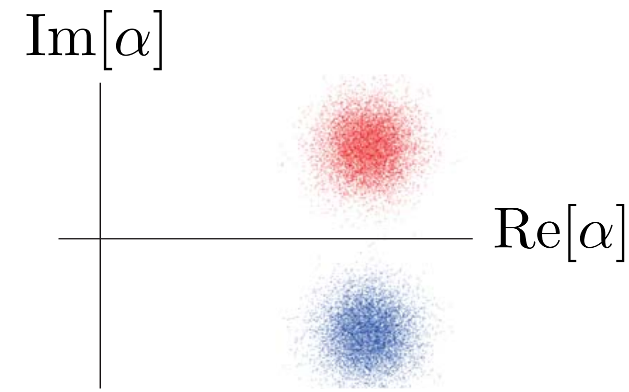

…by Photon Counting:

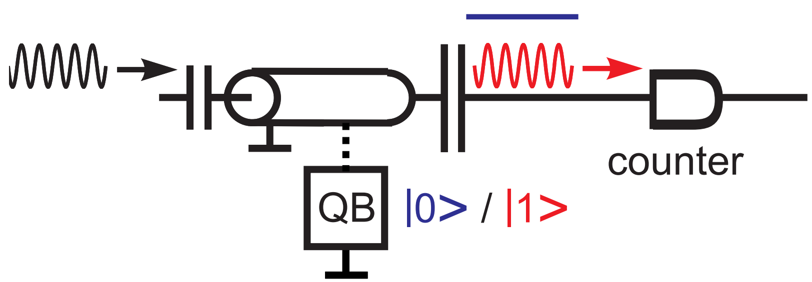

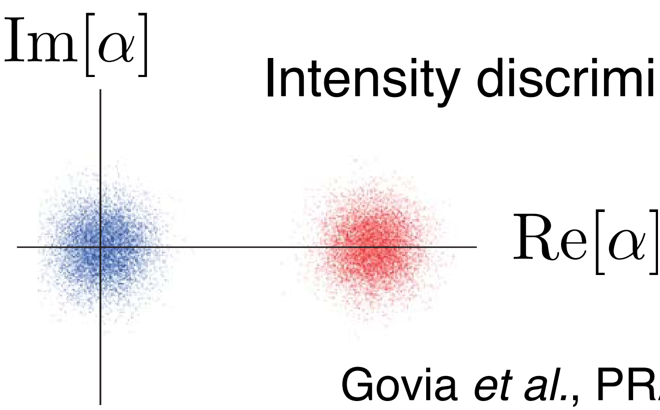

Intensity discrimination

Govia *et al.*, PRA **90**, 062307 (2014)

Govia *et al.*, PRA **92**, 022335 (2015)

Josephson Photomultiplier (JPM)

Chen *et al.*, PRL **107**, 217401 (2011)

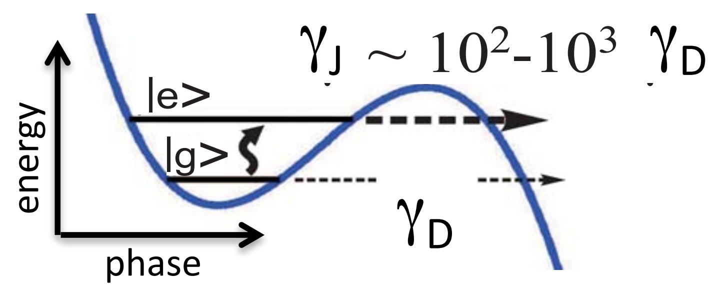

Tunneling events produce easily-measured, unambiguous “clicks”.

Photon-capture approach for JPM-based readout

*Opremcak *et al.*, Science 361, 1239 (2018)

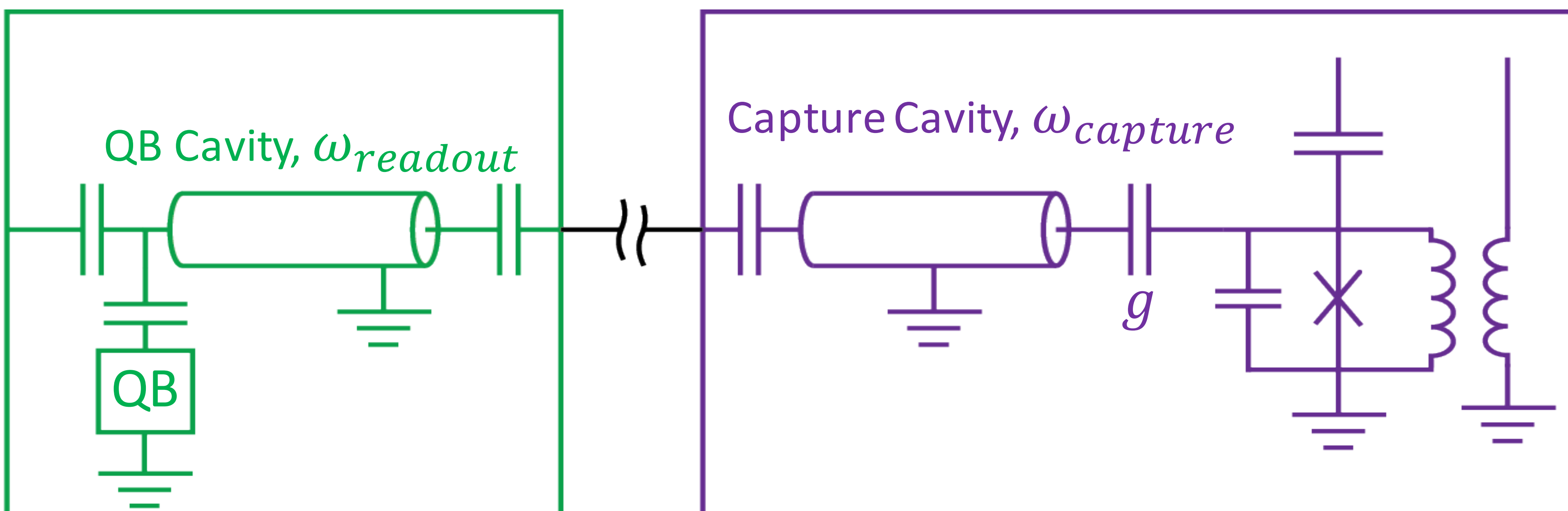

Qubit and JPM device fabrication

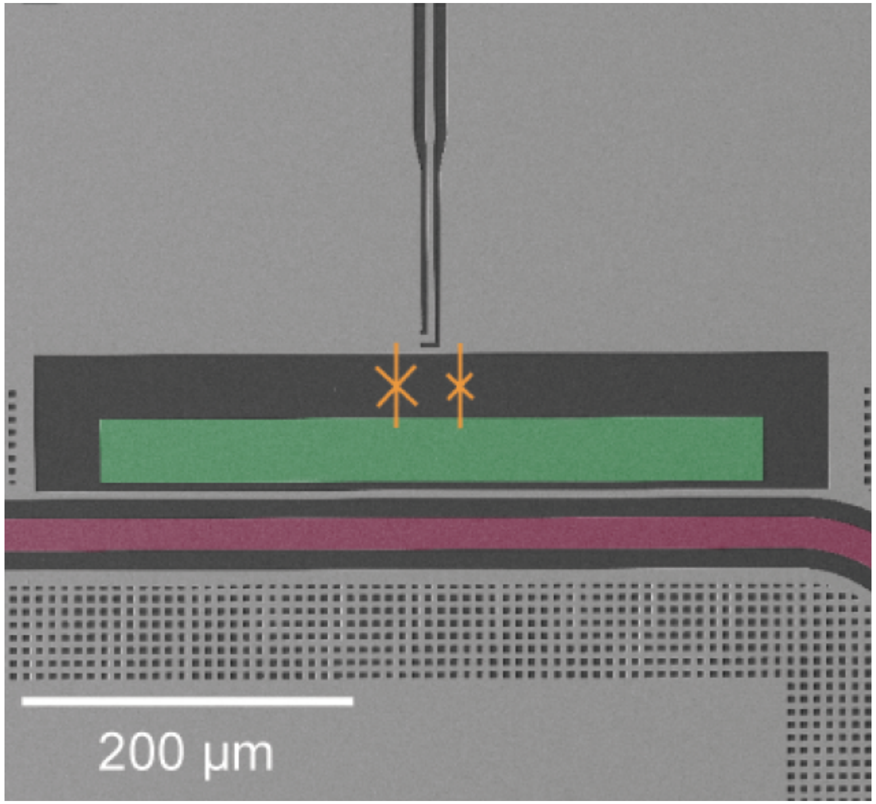

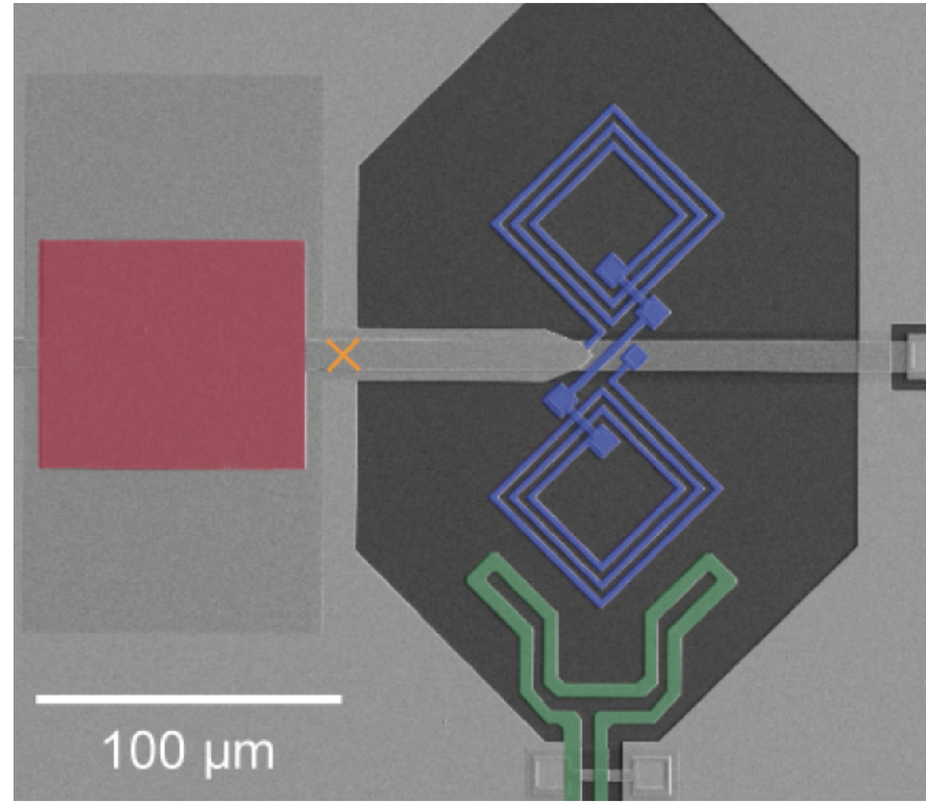

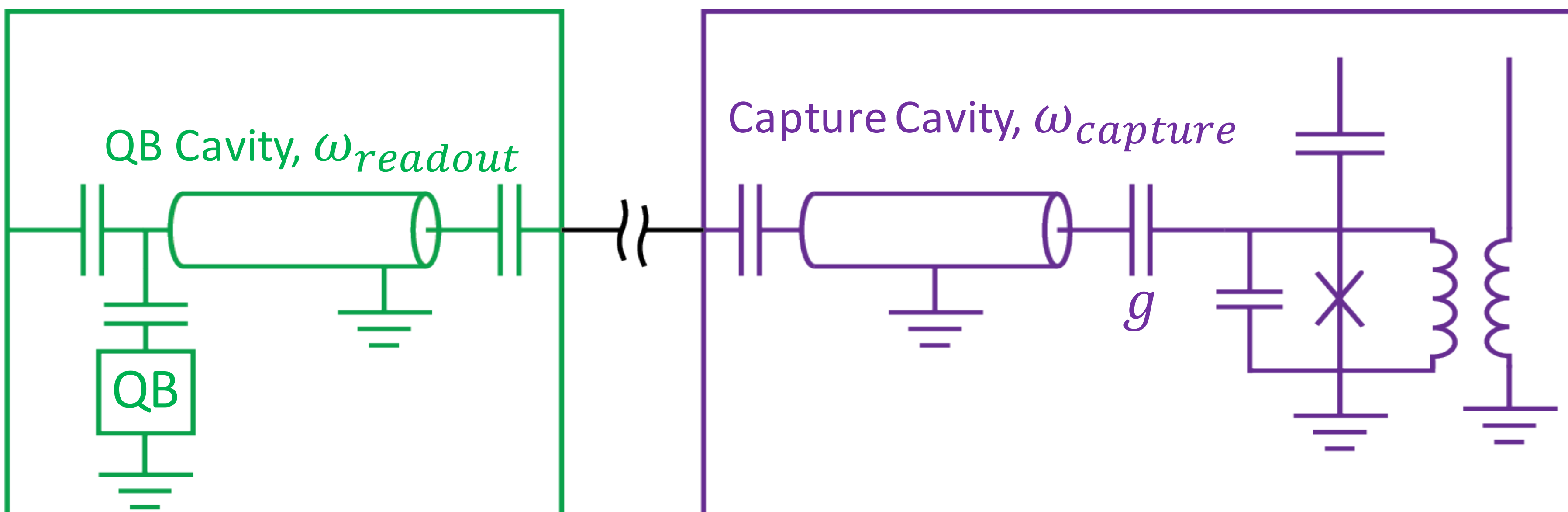

Interfacing JPM output with SFQ logic

- Qubit measurement result encoded in classical circulating current states of JPM
- Inductively couple JPM loop to Josephson Transmission Line
- Sense of circulating currents results in state-dependent delay of SFQ pulses

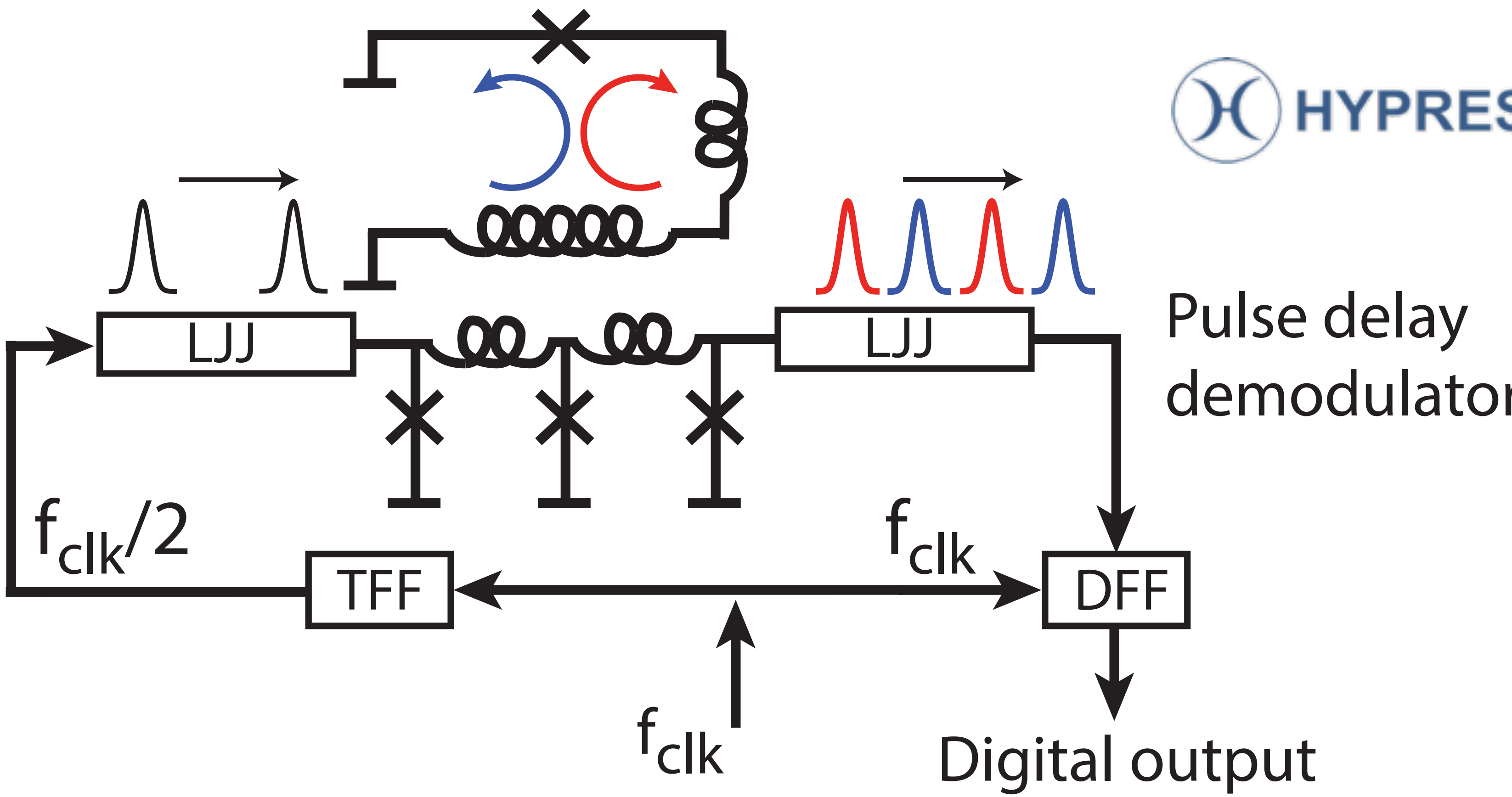

*A. Herr et al., *Superconductor Sci. Tech. 20, S450 (2007)*

*McDermott *et al.*, Quant. Sci. Tech. 3, 024004 (2018)

JPM signal

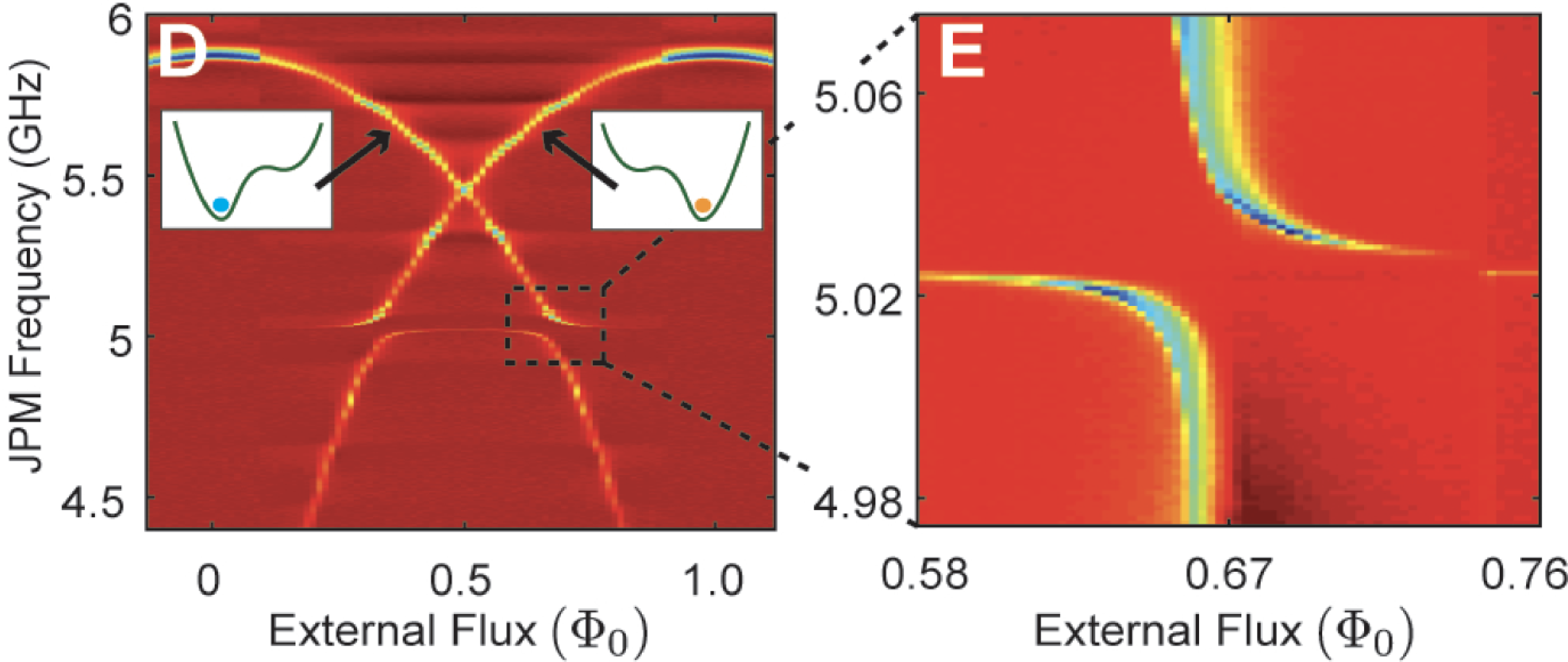

D
E
JPM Frequency (GHz)
6
5.5
5
4.5
0
0.5
1.0
External Flux (Φ_0)
5.06
5.02
4.98
0.58
0.67
0.76
External Flux (Φ_0)

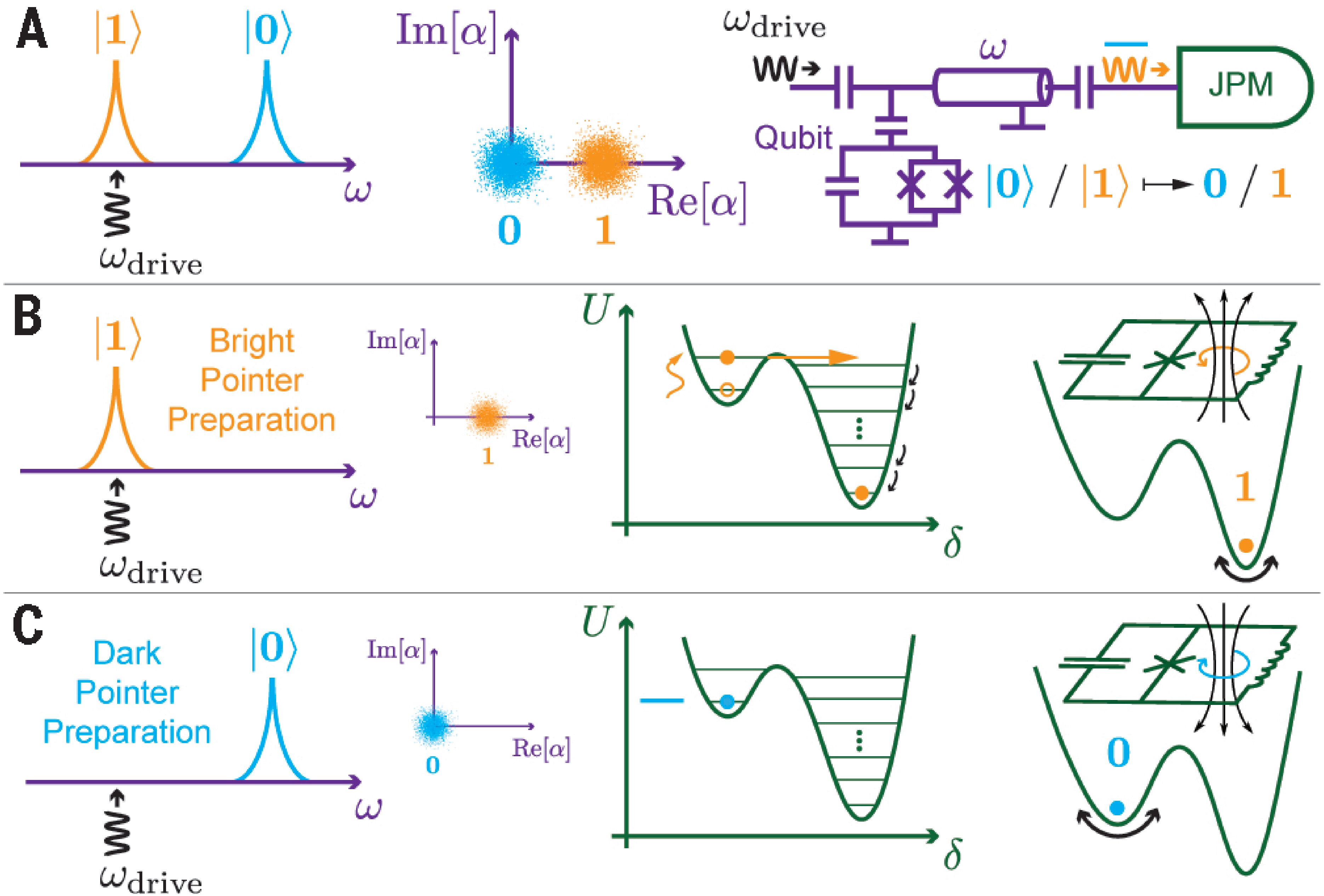
A
|1⟩
|0⟩
ω
ω_drive
Im[α]
Re[α]
0
1
ω_drive
ω
JPM
Qubit
|0⟩ / |1⟩ ↦ 0 / 1
B
|1⟩
Bright
Pointer
Preparation
Im[α]
Re[α]
1
U
δ
ω
ω_drive
C
Dark
Pointer
Preparation
|0⟩
ω
ω_drive
Im[α]
Re[α]
0
U
δ

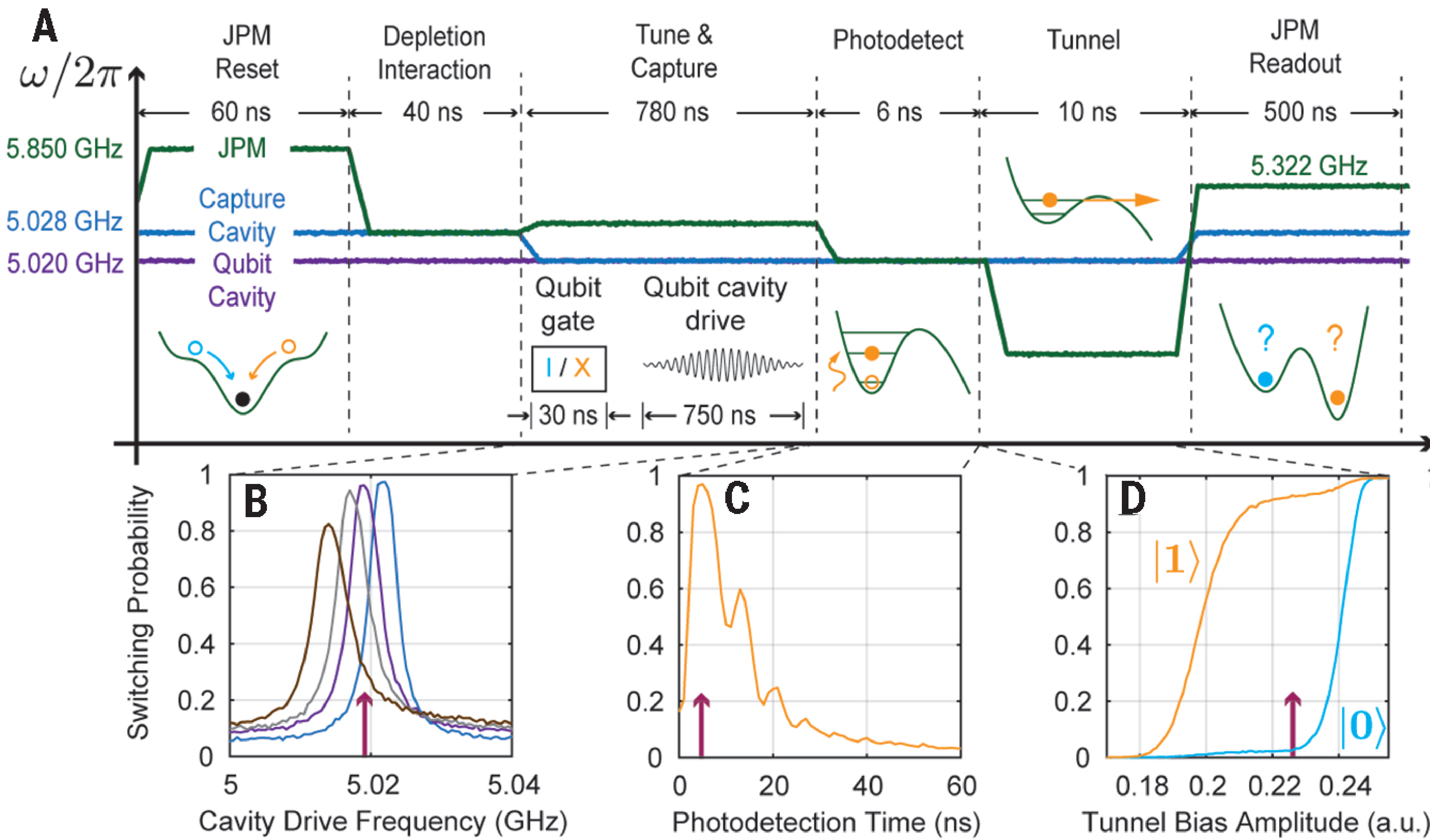

A
JPM Reset
Depletion Interaction
Tune & Capture
Photodetect
Tunnel
JPM Readout
ω/2π
60 ns
40 ns
780 ns
6 ns
10 ns
500 ns
5.850 GHz
JPM
5.322 GHz
Capture Cavity
5.028 GHz
5.020 GHz
Qubit Cavity
Qubit gate
I / X
Qubit cavity drive
30 ns
750 ns
?
?
t
B
C
D
Switching Probability
Cavity Drive Frequency (GHz)
Photodetection Time (ns)
Tunnel Bias Amplitude (a.u.)
|1⟩
|0⟩